were also positive for CXCL12. In addition, fibroblasts adjacent to cancer cells, as well as normal areas, were weakly positive, but their expression was significantly weaker than that of tumor cells. CXCL12 staining was localized diffusely or patchily, and CXCL12 was often expressed in tumor buds at the invasive front **Image 1B**.

The mean ± SD proportion of CXCL12+ tumor cells was 60.8% ± 27.3%. Of the 165 cases, 120 (72.7%) exhibited immunopositivity in 50% or more of the cancer cells.

Patients whose tumors had high CXCL12 expression had significantly shorter survival than patients whose tumors had low CXCL12 expression ($P = .014$ and $P = .005$, overall and recurrence-free survival rates, respectively; log-rank test) **Figure 1**. The correlations between the percentage of CXCL12 immunopositivity and clinicopathologic findings are shown in Table 1. The percentage of CXCL12 immunopositivity was correlated with the depth of tumor invasion, tumor budding grade determined by H&E staining, and liver metastasis.

The results of univariate analysis using the Cox proportional hazards model are shown in **Table 2**. CXCL12 expression was found to be a significant prognostic factor for overall and recurrence-free survival, together with depth of tumor invasion, tumor budding grade by H&E staining, and lymph node metastasis. In addition, blood vessel invasion was found to be a significant predictive factor for recurrence, whereas lymphatic vessel invasion tended to be predictive of recurrence. Multivariate analysis using the Cox proportional hazards model revealed that the percentage of CXCL12 immunopositivity and lymph node metastasis were independent prognostic factors for overall and recurrence-free survival **Table 3**.

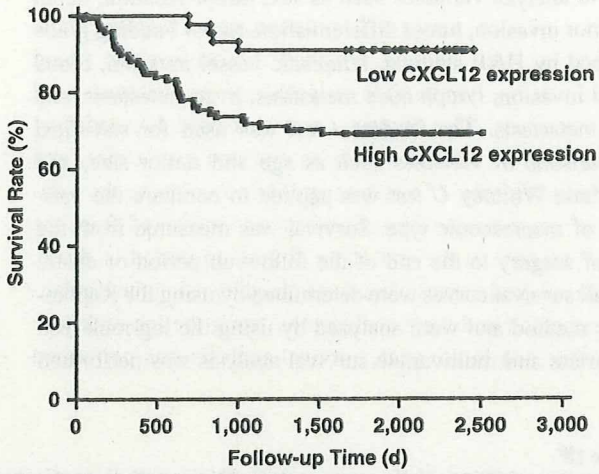

Figure 1 Kaplan-Meier survival curves of patients with colorectal carcinoma subdivided according to the proportion of tumor cells expressing CXCL12 ($P = .014$; log-rank test).

Grade of CXCL12 Immunopositivity in Foci of Tumor Budding

Of the 165 cases, 71 (43.0%) were defined as high grade, and the survival of the patients was significantly shorter than that of patients with low-grade tumors ($P = .003$ and $P < .001$, overall and recurrence-free survival rates, respectively; log-rank test) **Figure 2**. The number of CXCL12+ budding foci was correlated with the depth of tumor invasion ($P < .001$), tumor budding grade by H&E

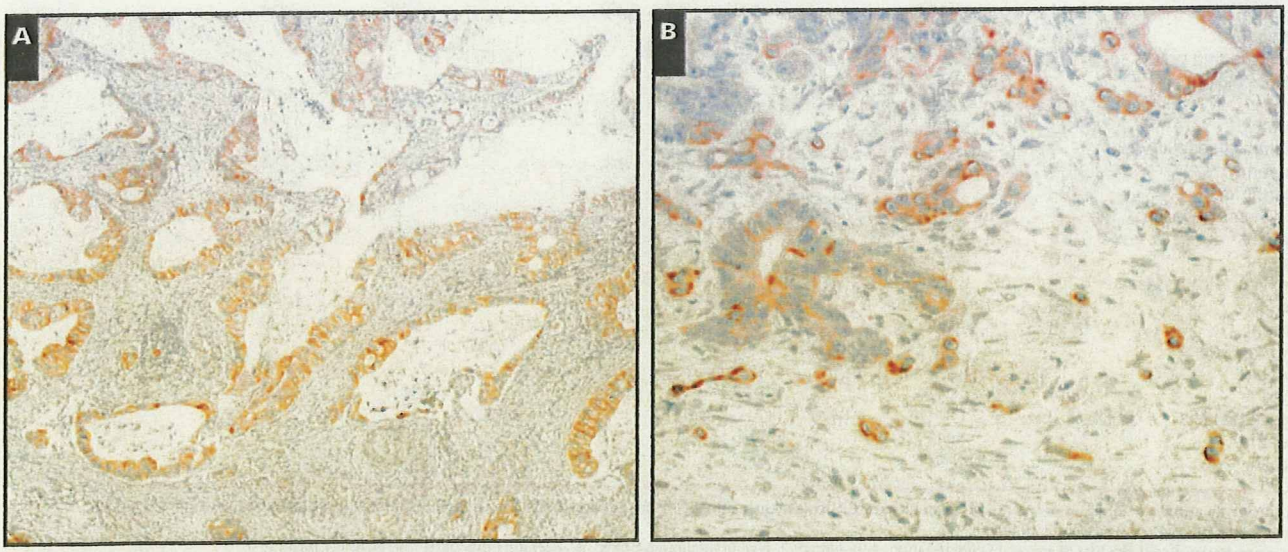

Image 1 Immunohistochemical studies of CXCL12 in colorectal carcinoma. **A**, CXCL12 expression was observed in the cell membrane and cytoplasm of colorectal tumor cells. In this case, almost all tumor cells expressed CXCL12 (×45). **B**, CXCL12 expression was intense in tumor budding foci at the invasive front (×230).

DOI: 10.1309/AJCPK35VZJEWCUTL

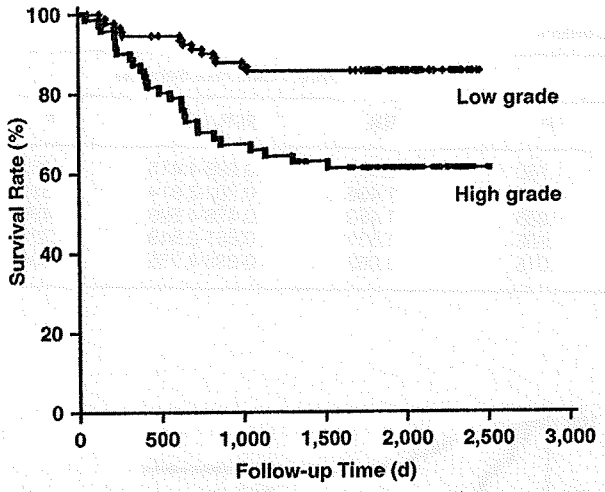

Figure 2 Kaplan-Meier survival curves of patients with colorectal carcinoma subdivided according to the grade of CXCL12+ tumor budding ($P = .003$; log-rank test).

staining ($P < .001$), lymph node metastasis ($P = .003$), and lung metastasis ($P = .030$) (Table 1). Univariate analysis using the Cox proportional hazards model revealed that the grade of CXCL12-immunopositive tumor budding was a significant prognostic factor (Table 2). Multivariate analysis using the Cox proportional hazards model revealed that only lymph node metastasis was an independent prognostic factor for overall survival and that CXCL12+ tumor budding grade was not an independent factor for overall or recurrence-free survival **Table 4**.

Combination of CXCL12 Expression and CXCL12+ Tumor Budding Grade

Patients with high CXCL12 expression and high-grade tumors had significantly shorter survival than patients with other combinations ($P < .001$ and $P < .001$, overall and recurrence-free survival rates, respectively; log-rank test) **Figure 3**. This combination was correlated with the depth of tumor invasion ($P < .001$), tumor budding grade by H&E

Table 2
Univariate Cox Proportional Hazards Analysis for the Candidate Variables*

	Overall Survival			Recurrence-Free Survival		
Prognostic Factor	**HR**	**95% CI**	***P***	**HR**	**95% CI**	***P***
CXCL12 expression	3.992	1.210-13.167	.023	3.991	1.420-11.219	.009
CXCL12+ tumor budding grade	3.036	1.420-6.493	.004	3.140	1.619-6.091	.001
CXCL12 expression and CXCL12+ tumor budding grade	3.540	1.655-7.574	.001	3.659	1.886-7.098	<.001
Age	1.013	0.538-1.906	.969	0.949	0.464-1.941	.885
Sex	1.139	0.609-2.133	.684	1.855	0.826-4.168	.134
Tumor location	1.118	0.573-2.430	.653	1.139	0.609-2.133	.684
Tumor size	1.119	0.546-2.293	.760	0.889	0.478-1.654	.711
Macroscopic type	0.977	0.278-3.429	.970	1.218	0.382-3.885	.740
Tumor depth (T2, T3 vs T4)	2.375	1.158-4.867	.018	2.442	1.312-4.544	.005
Tumor differentiation (grade 1/2 vs grade 3/4)	0.406	0.097-1.706	.219	0.556	0.134-2.307	.419
Tumor budding grade (H&E staining)	2.663	1.292-5.486	.008	2.230	1.198-4.150	.011
Lymphatic vessel invasion	2.032	0.709-5.824	.187	2.789	0.992-7.839	.052
Blood vessel invasion	2.081	0.893-4.853	.090	2.516	1.159-5.463	.020
Lymph node metastasis	5.454	1.902-15.639	.002	3.326	1.532-7.222	.002

HR, hazard ratio; CI, confidence interval.
* For descriptions of macroscopic type, tumor depth, and tumor differentiation, see the footnotes for Table 1.

Table 3
Multivariate Cox Proportional Hazards Analysis for the Candidate Variables

	Overall Survival			Recurrence-Free Survival		
Prognostic Factor	**HR**	**95% CI**	***P***	**HR**	**95% CI**	***P***
CXCL12 expression	4.138	1.209-14.168	.024	4.084	1.404-11.878	.010
Tumor depth*	1.332	0.621-2.856	.462	1.393	0.724-2.682	.321
Tumor budding grade (H&E staining)	1.354	0.616-2.975	.451	1.117	0.567-2.200	.750
Lymphatic vessel invasion	1.047	0.323-3.398	.939	1.576	0.516-4.810	.424
Blood vessel invasion	1.179	0.461-3.019	.731	1.535	0.657-3.582	.322
Lymph node metastasis	5.063	1.654-15.493	.005	2.781	1.200-6.444	.017

HR, hazard ratio; CI, confidence interval.
* For description, see the footnotes for Table 1.

DOI: 10.1309/AJCPK35VZJEWCUTL

Table 4
Multivariate Cox Proportional Hazards Analysis for the Candidate Variables

Prognostic Factor	Overall Survival			Recurrence-Free Survival		
	HR	95% CI	*P*	HR	95% CI	*P*
CXCL12+ tumor budding grade	1.859	0.782-4.417	.160	2.099	0.998-4.415	.051
Tumor depth*	1.422	0.624-3.242	.402	1.406	0.702-2.814	.336
Lymphatic vessel invasion	0.990	0.305-3.215	.986	1.483	0.478-4.598	.495
Blood vessel invasion	1.278	0.505-3.238	.605	1.531	0.661-3.549	.320
Lymph node metastasis	3.987	1.302-12.212	.015	2.052	0.886-4.755	.094

HR, hazard ratio; CI, confidence interval.
* For description, see the footnotes for Table 1.

staining ($P < .001$), lymph node metastasis ($P = .022$), and lung metastasis ($P = .014$). In addition, it showed a tendency to be correlated with liver metastasis ($P = .052$) (Table 1). Univariate analysis using the Cox proportional hazards model revealed that the combination of CXCL12 expression and CXCL12+ tumor budding grade was a significant prognostic factor (Table 2). Multivariate analysis using the Cox proportional hazards model revealed that the combination of CXCL12 expression and CXCL12+ tumor budding grade was an independent and significant prognostic factor for overall survival, together with lymph node metastasis, and also an independent prognostic factor for recurrence **Table 5**.

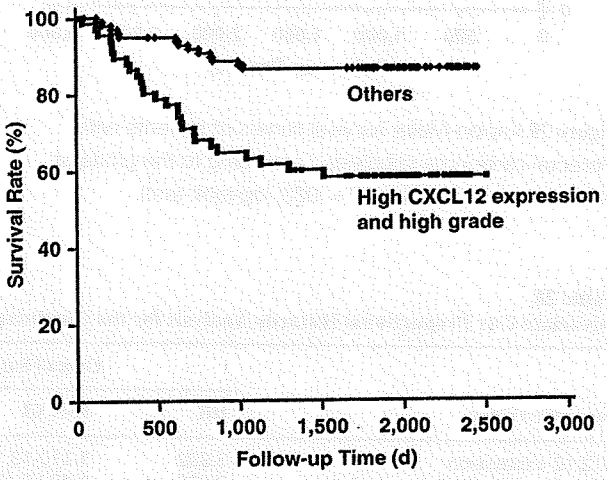

Figure 3 Kaplan-Meier survival curves of patients with colorectal carcinoma subdivided according to the combination of the proportion of CXCL12 expression and the grade of CXCL12+ tumor budding ($P < .001$; log-rank test).

Discussion

CXCL12 expression in colorectal cancer cells and at foci of tumor budding was found to be an independent predictive factor for cancer recurrence and poor survival. The present study indicated that CXCL12 expression in tumor cells was correlated with liver metastasis and was an independent prognostic factor together with lymph node metastasis. As it has been demonstrated that CXCL12 promotes tumor growth and malignancy,[21] colorectal cancers exhibiting high CXCL12 expression seem to show aggressive biologic behavior, with poor patient survival. To our knowledge, correlations between CXCL12 expression and long-term survival have been recognized in breast carcinoma,[21] ovarian

Table 5
Multivariate Cox Proportional Hazards Analysis for the Candidate Variables

Prognostic Factor	Overall Survival			Recurrence-Free Survival		
	HR	95% CI	*P*	HR	95% CI	*P*
CXCL12 expression and CXCL12+ tumor budding grade	2.48	1.065-5.776	.035	2.713	1.313-5.605	.007
Tumor depth*	1.261	0.556-2.860	.579	1.28	0.639-2.562	.486
Lymphatic vessel invasion	1.061	0.324-3.478	.922	1.571	0.504-4.892	.436
Blood vessel invasion	1.26	0.496-3.203	.627	1.51	0.650-3.504	.338
Lymph node metastasis	3.932	1.296-11.929	.016	2.056	0.895-4.721	.089

HR, hazard ratio; CI, confidence interval.
* For description, see the footnotes for Table 1.

DOI: 10.1309/AJCPK35VZJEWCUTL

carcinoma,[19] glioma,[20] esophageal carcinoma,[17] and gastric carcinoma.[18] Immunohistochemical staining of frozen breast cancer tissues has demonstrated CXCL12 mostly in tumor cells and stromal cells, and the level of CXCL12 transcription in the tumor is correlated significantly with overall survival and incidence-free survival.[21] In addition, in this study, we noted that CXCL12 expression was stronger at the invasive front than in other areas of colorectal cancer, reflecting the fact that the invasive front shows the most active interaction between cancer and stroma. We therefore further focused on CXCL12 expression at sites of tumor budding.

Tumor budding has been reported to be related to metastatic activity[27,28] and prognostic outcome.[26,29] Although previous studies have addressed the prognostic impact of tumor budding, the assessment of tumor budding was done by counting tumor budding foci[24,25,30] or scoring the degree of tumor budding.[29,31,32] However, for objective quantification of tumor budding, it is necessary to apply immunostaining with the keratin cocktail AE1/AE3 and/or low-molecular-weight keratins (CAM5.2 [cytokeratins 8 and 18]). This approach highlights tumor buds extremely well and allows easy selection of counting areas and easy and rapid counting.[24,31] However, immunostaining with AE1/AE3 and/or CAM5.2 does not reflect the biologic activity of the tumor because all of the tumor cells are immunopositive.

In this study, we were able to count the numbers of tumor budding foci more easily than by H&E staining by using immunohistochemical analysis for CXCL12. CXCL12 immunostaining was used not only to highlight tumor cells but also to examine their potential aggressiveness by counting the number that were CXCL12+. CXCL12+ tumor budding grade was also correlated with the depth of tumor invasion, tumor budding grade determined by H&E staining, lymph node metastasis, and lung metastasis. CXCL12+ tumor budding grade was also demonstrated to be a prognostic indicator for overall survival and recurrence, although multivariate analysis showed that it was not an independent factor.

One reason why CXCL12+ tumor budding grade was not an independent factor may have been that the grade was judged in only 1 area where the budding foci were most intense and, therefore, probably did not reflect the properties of the whole tumor. Therefore, we combined the grading of CXCL12 immunopositivity for tumor buds with the proportion of tumor cells expressing CXCL12. We found that patients whose tumors showed high CXCL12 expression and high grade had the worst outcome. The combination of CXCL12 expression and CXCL12+ tumor budding grade was further correlated with the depth of tumor invasion, tumor budding grade determined by H&E staining, lymph node metastasis, and lung metastasis and tended to be correlated with liver metastasis. Moreover, this combination was an independent and significant prognostic factor for overall survival, together with lymph node metastasis, and also an independent prognostic factor for recurrence.

In our study, only a few grade 3 and 4 cases (5 of 165 cases) were included. Therefore, it seems possible that tumor differentiation did not affect the results of analyses. In general, the majority of colorectal carcinomas are diagnosed as grade 1 or 2, and the majority of grade 3 or 4 cases are included among cases that are more advanced than stage II or III.

In the present study, CXCL12 was expressed distinctly in colorectal cancer cells, normal epithelium of the colon (especially in the middle to upper third of each crypt in the mucosal layer), and blood and lymphatic endothelial cells and weakly in fibroblasts. Previous reports indicated that CXCL12 was constitutively expressed in various organs, including lymph nodes, lung, liver, thymus, and stromal cells such as fibroblasts, endothelial cells, and osteoblasts in bone marrow.[4,6,12]

Multiple biologic activities of CXCL12 have also been described.[7-10] For example, in vitro studies have shown that CXCL12 can modulate tumor cell proliferation and migration.[11,33,34] CXCL12 probably stimulates the formation of capillary-like structures by human vascular endothelial cells.[9,35,36] In addition, hypoxia-dependent up-regulation of the chemokine receptor CXCR4 practically promotes breast cancer invasion and organ-specific metastasis.[37,38] Colorectal carcinoma cells, especially those at the invasive front, are likely to be situated in a hypoxic milieu.[39,40] Therefore, this may lead to further tumor invasion through up-regulation of CXCL12/CXCR4.

CXCL12 expression in colorectal cancer cells and the grading of CXCL12 immunopositivity at foci of tumor budding are each significant prognostic factors. However, our present results suggest that, in colorectal carcinoma, CXCL12 expression used in combination with tumor budding grade is a more powerful prognostic indicator than either factor alone.

From the [1]Pathology Division, National Cancer Center Research Institute, Tokyo, Japan; and [2]Surgery Division, National Cancer Center Hospital, Tokyo.

Supported in part by a Grant-in-Aid for the Third Term Comprehensive 10-Year Strategy for Cancer Control from the Ministry of Health, Labour and Welfare of Japan and grant 19790275 from the Ministry of Education, Culture, Sports, Science, and Technology of Japan.

Address reprint requests to Dr Akishima-Fukasawa: Pathology Division, National Cancer Center Research Institute, 5-1-1 Tsukiji, Chuo-ku, Tokyo 104-0045, Japan.

DOI: 10.1309/AJCPK35VZJEWCUTL

References

1. Ottaiano A, Franco R, Aiello Talamanca A, et al. Overexpression of both CXC chemokine receptor 4 and vascular endothelial growth factor proteins predicts early distant relapse in stage II-III colorectal cancer patients. *Clin Cancer Res.* 2006;12:2795-2803.
2. Liotta LA, Kohn EC. The microenvironment of the tumour-host interface. *Nature.* 2001;411:375-379.
3. Ibe S, Qin Z, Schuler T, et al. Tumor rejection by disturbing tumor stroma cell interactions. *J Exp Med.* 2001;194:1549-1559.
4. Shirozu M, Nakano T, Inazawa J, et al. Structure and chromosomal localization of the human stromal cell-derived factor 1 (*SDF1*) gene. *Genomics.* 1995;28:495-500.
5. Nagasawa T, Kikutani H, Kishimoto T. Molecular cloning and structure of a pre-B-cell growth-stimulating factor. *Proc Natl Acad Sci U S A.* 1994;91:2305-2309.
6. Tashiro K, Tada H, Heilker R, et al. Signal sequence trap: a cloning strategy for secreted proteins and type I membrane proteins. *Science.* 1993;261:600-603.
7. Fernandis AZ, Prasad A, Band H, et al. Regulation of CXCR4-mediated chemotaxis and chemoinvasion of breast cancer cells. *Oncogene.* 2004;23:157-167.
8. Nagasawa T, Tachibana K, Kishimoto T. A novel CXC chemokine PBSF/SDF-1 and its receptor CXCR4: their functions in development, hematopoiesis and HIV infection. *Semin Immunol.* 1998;10:179-185.
9. Salcedo R, Wasserman K, Young HA, et al. Vascular endothelial growth factor and basic fibroblast growth factor induce expression of CXCR4 on human endothelial cells: in vivo neovascularization induced by stromal-derived factor-1alpha. *Am J Pathol.* 1999;154:1125-1135.
10. Tachibana K, Hirota S, Iizasa H, et al. The chemokine receptor CXCR4 is essential for vascularization of the gastrointestinal tract. *Nature.* 1998;393:591-594.
11. Phillips RJ, Burdick MD, Lutz M, et al. The stromal derived factor-1/CXCL12-CXC chemokine receptor 4 biological axis in non-small cell lung cancer metastases. *Am J Respir Crit Care Med.* 2003;167:1676-1686.
12. Muller A, Homey B, Soto H, et al. Involvement of chemokine receptors in breast cancer metastasis. *Nature.* 2001;410:50-56.
13. Zeelenberg IS, Ruuls-Van Stalle L, Roos E. The chemokine receptor CXCR4 is required for outgrowth of colon carcinoma micrometastases. *Cancer Res.* 2003;63:3833-3839.
14. Schimanski CC, Schwald S, Simiantonaki N, et al. Effect of chemokine receptors CXCR4 and CCR7 on the metastatic behavior of human colorectal cancer. *Clin Cancer Res.* 2005;11:1743-1750.
15. Kaifi JT, Yekebas EF, Schurr P, et al. Tumor-cell homing to lymph nodes and bone marrow and CXCR4 expression in esophageal cancer. *J Natl Cancer Inst.* 2005;97:1840-1847.
16. Taichman RS, Cooper C, Keller ET, et al. Use of the stromal cell-derived factor-1/CXCR4 pathway in prostate cancer metastasis to bone. *Cancer Res.* 2002;62:1832-1837.
17. Sasaki K, Natsugoe S, Ishigami S, et al. Expression of CXCL12 and its receptor CXCR4 correlates with lymph node metastasis in submucosal esophageal cancer. *J Surg Oncol.* 2008;97:433-438.
18. Ishigami S, Natsugoe S, Okumura H, et al. Clinical implication of CXCL12 expression in gastric cancer. *Ann Surg Oncol.* 2007;14:3154-3158.
19. Jiang YP, Wu XH, Shi B, et al. Expression of chemokine CXCL12 and its receptor CXCR4 in human epithelial ovarian cancer: an independent prognostic factor for tumor progression. *Gynecol Oncol.* 2006;103:226-233.
20. Salmaggi A, Gelati M, Pollo B, et al. CXCL12 expression is predictive of a shorter time to tumor progression in low-grade glioma: a single-institution study in 50 patients. *J Neurooncol.* 2005;74:287-293.
21. Kang H, Watkins G, Parr C, et al. Stromal cell derived factor-1: its influence on invasiveness and migration of breast cancer cells in vitro, and its association with prognosis and survival in human breast cancer. *Breast Cancer Res.* 2005;7:R402-R410.
22. Sobin L, Wittekind C; for the International Union Against Cancer (UICC), eds. *TNM Classification of Malignant Tumours.* 6th ed. New York, NY: Wiley-Liss; 2002.
23. Hamilton SR, Aaltonen LA. *Pathology and Genetics of Tumours of the Digestive System.* Lyon, France: IARC Press; 2000. *World Health Organization Classification of Tumours.*
24. Prall F, Nizze H, Barten M. Tumour budding as prognostic factor in stage I/II colorectal carcinoma. *Histopathology.* 2005;47:17-24.
25. Ueno H, Price AB, Wilkinson KH, et al. A new prognostic staging system for rectal cancer. *Ann Surg.* 2004;240:832-839.
26. Ueno H, Murphy J, Jass JR, et al. Tumour "budding" as an index to estimate the potential of aggressiveness in rectal cancer. *Histopathology.* 2002;40:127-132.
27. Okuyama T, Oya M, Ishikawa H. Budding as a risk factor for lymph node metastasis in pT1 or pT2 well-differentiated colorectal adenocarcinoma. *Dis Colon Rectum.* 2002;45:628-634.
28. Goldstein NS, Hart J. Histologic features associated with lymph node metastasis in stage T1 and superficial T2 rectal adenocarcinomas in abdominoperineal resection specimens: identifying a subset of patients for whom treatment with adjuvant therapy or completion abdominoperineal resection should be considered after local excision. *Am J Clin Pathol.* 1999;111:51-58.
29. Hase K, Shatney C, Johnson D, et al. Prognostic value of tumor "budding" in patients with colorectal cancer. *Dis Colon Rectum.* 1993;36:627-635.
30. Ueno H, Mochizuki H, Hashiguchi Y, et al. Predictors of extrahepatic recurrence after resection of colorectal liver metastases. *Br J Surg.* 2004;91:327-333.
31. Kazama S, Watanabe T, Ajioka Y, et al. Tumour budding at the deepest invasive margin correlates with lymph node metastasis in submucosal colorectal cancer detected by anticytokeratin antibody CAM5.2. *Br J Cancer.* 2006;94:293-298.
32. Nakamura T, Mitomi H, Kikuchi S, et al. Evaluation of the usefulness of tumor budding on the prediction of metastasis to the lung and liver after curative excision of colorectal cancer. *Hepatogastroenterology.* 2005;52:1432-1435.
33. Brand S, Dambacher J, Beigel F, et al. CXCR4 and CXCL12 are inversely expressed in colorectal cancer cells and modulate cancer cell migration, invasion and MMP-9 activation. *Exp Cell Res.* 2005;310:117-130.
34. Scotton CJ, Wilson JL, Scott K, et al. Multiple actions of the chemokine CXCL12 on epithelial tumor cells in human ovarian cancer. *Cancer Res.* 2002;62:5930-5938.
35. Salcedo R, Oppenheim JJ. Role of chemokines in angiogenesis: CXCL12/SDF-1 and CXCR4 interaction, a key regulator of endothelial cell responses. *Microcirculation.* 2003;10:359-370.
36. Mirshahi F, Pourtau J, Li H, et al. SDF-1 activity on microvascular endothelial cells: consequences on angiogenesis in in vitro and in vivo models. *Thromb Res.* 2000;99:587-594.

DOI: 10.1309/AJCPK35VZJEWCUTL

37. Phillips RJ, Mestas J, Gharaee-Kermani M, et al. Epidermal growth factor and hypoxia-induced expression of CXC chemokine receptor 4 on non-small cell lung cancer cells is regulated by the phosphatidylinositol 3-kinase/PTEN/AKT/mammalian target of rapamycin signaling pathway and activation of hypoxia inducible factor-1alpha. *J Biol Chem.* 2005;280:22473-22481.
38. Matteucci E, Locati M, Desiderio MA. Hepatocyte growth factor enhances CXCR4 expression favoring breast cancer cell invasiveness. *Exp Cell Res.* 2005;310:176-185.
39. Sullivan R, Graham CH. Hypoxia-driven selection of the metastatic phenotype. *Cancer Metastasis Rev.* 2007;26:319-331.
40. Zhong H, De Marzo AM, Laughner E, et al. Overexpression of hypoxia-inducible factor 1alpha in common human cancers and their metastases. *Cancer Res.* 1999;59:5830-5835.

DOI: 10.1309/AJCPK35VZJEWCUTL

Clinical Translational Research

Oncology

Oncology 2009;77:53–62
DOI: 10.1159/000226112

Received: September 24, 2008
Accepted after revision: February 16, 2009
Published online: June 25, 2009

Podoplanin Expression Identified in Stromal Fibroblasts as a Favorable Prognostic Marker in Patients with Colorectal Carcinoma

Takahiro Yamanashi[a, c] Yukihiro Nakanishi[a] Gen Fujii[a] Yuri Akishima-Fukasawa[a]
Yoshihiro Moriya[b] Yae Kanai[a] Masahiko Watanabe[c] Setsuo Hirohashi[a]

[a]Pathology and [b]Surgery Divisions, National Cancer Center Research Institute and Hospital, Tokyo, and
[c]Department of Surgery, Kitasato University School of Medicine, Kanagawa, Japan

Key Words
Podoplanin · Colorectal cancer · Prognosis · Immunohistochemistry · Clinicopathologic study

Abstract
Objective: The microenvironment of cancer plays a critical role in its progression. However, the molecular features of cancer-associated fibroblasts (CAFs) are less well understood than those of cancer cells. We investigated the clinicopathological significance of podoplanin expression in stromal fibroblasts in patients with colorectal cancer (CRC). ***Methods:*** We selected podoplanin as an upregulated marker in CAF from a DNA microarray experiment. Consequently, podoplanin was identified as an upregulated gene. Immunohistochemical podoplanin expression was investigated at the National Cancer Center Hospital, Tokyo, Japan, in 120 patients with advanced CRC, and its clinicopathological significance was examined. The biological function of podoplanin expression was also assessed by a coculture invasion assay with CRC cell lines such as HCT116 and HCT15. ***Results:*** Podoplanin expression was exclusively confined to stromal fibroblasts and absent in tumor cells. Podoplanin is absent in normal stroma except for lymphatic vessels. Staining was considered positive when over 30% of the cancer stroma was stained. Positive podoplanin expression was significantly correlated with a more distal tumor localization ($p = 0.013$) and a shallower depth of tumor invasion ($p = 0.011$). Univariate analysis revealed that negative podoplanin expression in stromal fibroblasts was significantly associated with reduced disease-specific survival ($p = 0.0017$) and disease-free survival ($p < 0.0001$). Multivariate analysis revealed that negative podoplanin expression ($p = 0.016$) and lymph node metastasis ($p = 0.027$) were significantly associated with disease-free survival. CRC cell invasion was augmented by coculture with CAFs that were treated with siRNA for podoplanin. ***Conclusions:*** Our results suggest that a positive podoplanin expression in stromal fibroblasts could have a protective role against CRC cell invasion and is a significant indicator of a good prognosis in patients with advanced CRC, supported by biological analysis showing that podoplanin expression in CAFs is associated with decreased CRC cell invasion.

Introduction

Previous reports have indicated that tumor progression is influenced and controlled by cellular interaction derived from a complex relationship between stromal, epithelial, and extracellular matrix components [1–5].

KARGER
Fax +41 61 306 12 34
E-Mail karger@karger.ch
www.karger.com

0030–2414/09/0771–0053$26.00/0

Accessible online at:
www.karger.com/ocl

Yukihiro Nakanishi, MD, PhD
Department of Pathology, National Cancer Center Research Institute
5-1-1 Tsukiji, Chuo-ku, Tokyo 104-0045 (Japan)
Tel. +81 3 3542 2511, ext. 4206, Fax +81 3 3248 2463
E-Mail yukihironakanishi@hotmail.com

Studies of breast, prostate, colon cancer and melanoma have identified a 'reactive stroma' that is characterized by a modified extracellular matrix composition, increased microvessel density, and the presence of inflammatory cells and fibroblasts with an 'activated' phenotype [6–11]. These modified fibroblasts, often termed myofibroblasts or cancer-associated fibroblasts (CAFs), are considered to play a central role in the complex process of tumor-stroma interaction and consequent tumorigenesis [1–5]. Numerous studies have provided evidence for a cancer-promoting role of activated CAFs [1–5], which supposedly initiate and promote tumor progression through specific communications with cancer cells. On the other hand, some CAFs could have a protective role against colorectal cancer (CRC) cell invasion. Nevertheless, the signals that could explain the transition of a normal fibroblast into a CAF are not fully understood, and therefore it has been unclear how the stromal reaction in cancer tissue supports and regulates tumor progression.

Podoplanin is a 38-kDa mucin-type transmembrane glycoprotein with extensive O-glycosylation and a high content of sialic acid, and has been implicated in tumor progression [12–16]. Podoplanin homologs include OTS-8, RT140, gp38, canine gp40, human gp36, and murine PA2.26 [17]. Since podoplanin is expressed on lymphatic, but not on blood vessel endothelium, it is also widely used as a specific marker for lymphatic endothelial cells and lymphangiogenesis [18, 19]. It has been reported that podoplanin-deficient mice die at birth due to respiratory failure, exhibiting a phenotype of dilated, malfunctioning lymphatic vessels and lymphedema [20]. Experiments addressing this issue have revealed that podoplanin colocalizes with ezrin, ERM (ezrin-radixin-moesin)-protein, at the cellular membrane, and that podoplanin promotes relocalization of ezrin to filopodia-like structures and induces cell migration in the absence of epithelial-mesenchymal transition [21]. Additionally, there is evidence to suggest that podoplanin promotes platelet aggregation, and that it may also be involved in cancer cell migration, invasion, metastasis, and malignant progression [22, 23]. The expression of podoplanin is upregulated in a number of different tumor types, including squamous cell carcinoma [13, 24], malignant mesothelioma [25, 26], Kaposi's sarcoma and angiosarcoma [19], hemangioblastoma [27], testicular seminoma [28], and brain tumors [12, 29, 30]. However, the physiological function of podoplanin is still unknown. Also, the functional contribution of podoplanin to tumor progression has remained elusive. Only a few previous studies have investigated podoplanin in fibroblasts, where PA2.26 antigen, a podoplanin homolog, is involved in reactive processes during skin remodeling [31].

In the present study, we selected podoplanin as a good upregulated marker molecule in CAF from a DNA microarray experiment (data not shown). Podoplanin expression in advanced colorectal carcinoma was investigated immunohistochemically and its clinicopathological significance was examined. Furthermore, its function in fibroblasts was assessed by using a coculture invasion assay with CRC cell lines.

Patients and Methods

Patients and Samples for Immunohistochemistry

One hundred twenty formalin-fixed and paraffin-embedded blocks of CRC were drawn from the files of the National Cancer Center Hospital (NCCH), Tokyo, Japan. All cases were surgically resected between July 1, 1996, and January 1, 1998, and diagnosed as primary advanced CRC. The patients included 76 (63.3%) males and 44 (36.7%) females ranging in age from 31 to 86 years (median 60 years). The patients were restricted to consecutive cases diagnosed as stage II (n = 50, 41.7%) or stage III (n = 70, 58.3%) pathologically, in which all patients had undergone curative resection and none received pre- or postoperative adjuvant chemotherapy or radiation therapy. No patients were excluded from this study because of adjuvant therapy. Follow-up studies were complete in all patients, with a period ranging from 0.1 months to 6.6 years (median 5.2 years). Seven (14.0%) patients at stage II and 22 (31.4%) at stage III developed recurrences, and 3 (6.0%) patients at stage II and 16 (22.9%) at stage III died of CRC. Among the cases showing recurrences, liver metastasis was observed in 5 (10.0%) stage II cases and 12 (17.1%) stage III cases. Clinicopathological factors were all classified according to the TNM classification of the International Union against Cancer [32]. Histologic classification of tumors was made according to the World Health Organization International Histological Classification of Tumors [33]. Among the study cases, 41 (34.2%) were classified as well differentiated adenocarcinoma, 75 (62.5%) as moderately differentiated adenocarcinoma, 3 (2.5%) as poorly differentiated adenocarcinoma, and 1 (0.8%) as mucinous adenocarcinoma.

Immunohistochemistry

Four-micrometer-thick sections of tissue samples of the 120 CRCs were stained for the selected molecule, podoplanin, which was identified as being overexpressed in CAFs. Sections were deparaffinized in xylene and rehydrated in a graded ethanol series. Staining was done at room temperature as follows: all sections were quenched with 3% hydrogen peroxide solution in alcohol for 20 min to block endogenous peroxidase activity. After several washes in phosphate-buffered saline (PBS; Sigma, St. Louis, Mo., USA), the sections were heated in an autoclave to 121 °C for 10 min in 0.01 M citrate buffer (pH 6.0) for antigen retrieval. Blocking was performed with 2% normal swine serum (NSS; Dako, Glostrup, Denmark) in PBS for 30 min, and then the sections were incubated with monoclonal antibody directed against human podoplanin (anti-D2–40; Dako) for 1 h at 1:50 dilution. After washing

in PBS, the sections were incubated with biotinylated antibody against mouse immunoglobulin G (Vector Laboratories, Burlingame, Calif., USA) for 30 min at 1:200 dilution, followed by streptavidin-conjugated horseradish peroxidase (Dako). Diaminobenzidine was used as a chromogen. Sections were counterstained with hematoxylin and coverslipped using Promounter (Meisei Electric Co., Bangkok, Thailand). For the negative control, 2% NSS was used instead of the primary antibody. Lymphatic vessels in normal stroma were used as a positive control for podoplanin immunopositivity.

Evaluation of Podoplanin Expression in CRCs

Immunostained sections of the 120 CRCs were evaluated using a light microscope by two observers (T.Y. and Y.A-F.) who were blinded to the patient characteristics. Podoplanin was evaluated according to the following criteria: staining was considered positive when staining equal to or stronger than that of lymphatic vessels was observed; staining was considered negative when it was absent or weaker than that of lymphatic vessels. Positive staining was divided into two groups: group A showing positive staining of 30% or more of the cancer stroma, and group B showing staining of less than 30% of the cancer stroma. Cases that were negative for podoplanin expression were classified into group B.

Statistical Analysis for Immunohistochemistry

Statistical tests were performed with StatView version 5.0 (SAS, Cary, N.C., USA). The relationships between immunohistochemical findings and clinicopathological factors were analyzed using Fisher's exact test, the χ^2 test, Student's t test, or the Mann-Whitney U test. Deaths from causes other than CRC were treated as censored cases. Overall survival, recurrence-free survival, and liver metastasis-free survival were measured from the date of surgery to the end of follow-up, recurrence, liver metastasis and death, respectively. Survival curves were made using the Kaplan-Meier method and compared using the log rank test. Both univariate and multivariate survival analyses were performed using the Cox proportional hazards regression model.

Cell Culture

The human fibroblast cell line CCD-112CoN (CRL-1541) derived from normal colon tissue and the human CRC cell lines HT29, HCT116, and HCT15 were obtained from the American Type Culture Collection. CCD-112CoN cells were maintained in Eagle's Minimal Essential Medium (Gibco, Carlsbad, Calif., USA) supplemented with 10% fetal bovine serum (FBS; Gibco), 500 units/ml penicillin-streptomycin-fungizone (Gibco), 2 mmol/l L-glutamine (Gibco), and 1 mmol/l sodium pyruvate (Gibco). All CRC cell lines were maintained in RPMI-1640 medium (Sigma) supplemented with 10% FBS and antibiotics. All cell lines were cultured under conditions of 5% CO_2 in air at 37°C. CCD112CoN fibroblasts were used between the 25th and 30th passages for the experiments.

Preparation of Cancer-Conditioned Medium

Conditioned medium derived from cancer cell lines was used for induction of podoplanin in CAFs. After HT29 had been plated and allowed to attach to 75-cm^2 tissue culture dishes (Corning, Corning, N.Y., USA) for 24 h at subconfluency, the cells were rinsed twice with PBS and then incubated for another 72 h. The conditioned medium (CM) derived from HT29 (CM-HT29) was harvested, centrifuged at 200 *g* for 10 min to remove cell debris, and passed through a 0.2-μm filter (Millipore, Billerica, Mass., USA). Until use, the CM was stored at –20°C, which did not alter its biological activity (data not shown).

Design of siRNA and Its Use for Transfection

A siRNA duplex (sense, 5′-CAACAGUGUAACAGGCAUUdTdT-3′) specific for human podoplanin (GenBank accession No. NM_006474) was designed at Takara Bio Inc. (Shiga, Japan). Nonspecific control siRNA duplex with the same GC content as podoplanin siRNA (sense, 5′-AUACAGUGACAGCAACGUUdTdT-3′) was also purchased. Fibroblast cell line CCD-112CoN, in which podoplanin is not constitutively expressed in low-serum medium, was plated on 75-cm^2 tissue culture dishes in a subconfluent state. To create fibroblast cells expressing podoplanin, CCD-112CoN was allowed to adhere for 3 h in Eagle's Minimal Essential Medium with 10% FBS, washed twice with PBS and incubated in CM-HT29 with 10% FBS for 48 h. The cells were then plated on 6-well tissue culture plates at a density of 1.25×10^5 cells per well in CM-HT29 with 10% FBS. After overnight incubation, the cells were transfected with podoplanin siRNA or control siRNA at a final concentration of 100 nmol/l using LipofectAMINE 2000 (Invitrogen, Carlsbad, Calif., USA). For optimal transfection, a reduced serum medium (Opti-MEM; Gibco) was used to dilute the siRNA duplexes and LipofectAMINE 2000 according to the manufacturer's recommendations. Cells were used for Western blot analysis and Matrigel invasion assays after 72 h.

Western Blot Analysis

Cells were lysed in Tris-buffered saline-based lysis buffer (Tris-buffered saline, 1% Triton X-100, 0.5% sodium deoxycholate, 0.1% sodium lauryl sulfate, protease inhibitor), and protein concentration was determined using the Bio-Rad Protein Assay (Bio-Rad Laboratories, Hercules, Calif., USA). Equal amounts of proteins (10 μg) from the whole-cell lysates were separated by 10% SDS-PAGE and transferred to polyvinylidene difluoride membranes (Millipore). The membranes were blocked in TPBS (0.1% Tween 20 in PBS) solution with 5% nonfat dry milk for 1 h, then incubated with monoclonal antibody directed against human podoplanin (anti-D2–40; Dako) for 2 h at 1:100 dilution in blocking solution. Subsequently, the membranes were washed with TPBS, followed by incubation with horseradish-peroxidase-conjugated anti-mouse IgG antibody (GE Healthcare, Amersham, UK) for 1 h at 1:1,000 dilution. Immunoreactive proteins were detected using an enhanced chemiluminescence kit (GE Healthcare). β-Actin monoclonal antibody (Sigma) at 1:2,000 dilution was used as protein loading control.

Matrigel Invasion Assay

The transfected fibroblasts were cocultured with the invasive CRC cell lines (either HT116 or HT15) and analyzed using the BD BioCoat Matrigel Invasion Assay System (24-well BioCoat Matrigel invasion chambers; BD Bioscience, San Jose, Calif., USA) in accordance with the manufacturer's recommendations with minor modification. Briefly, after 24 h of transfection, the fibroblasts were plated on the upper chamber of the transwell insert (8-μm pores) in the presence or absence of CM-HT29 with 10% FBS at a density of 1×10^4 cells, and the lower wells contained the same medium. After overnight incubation, either HCT116 or

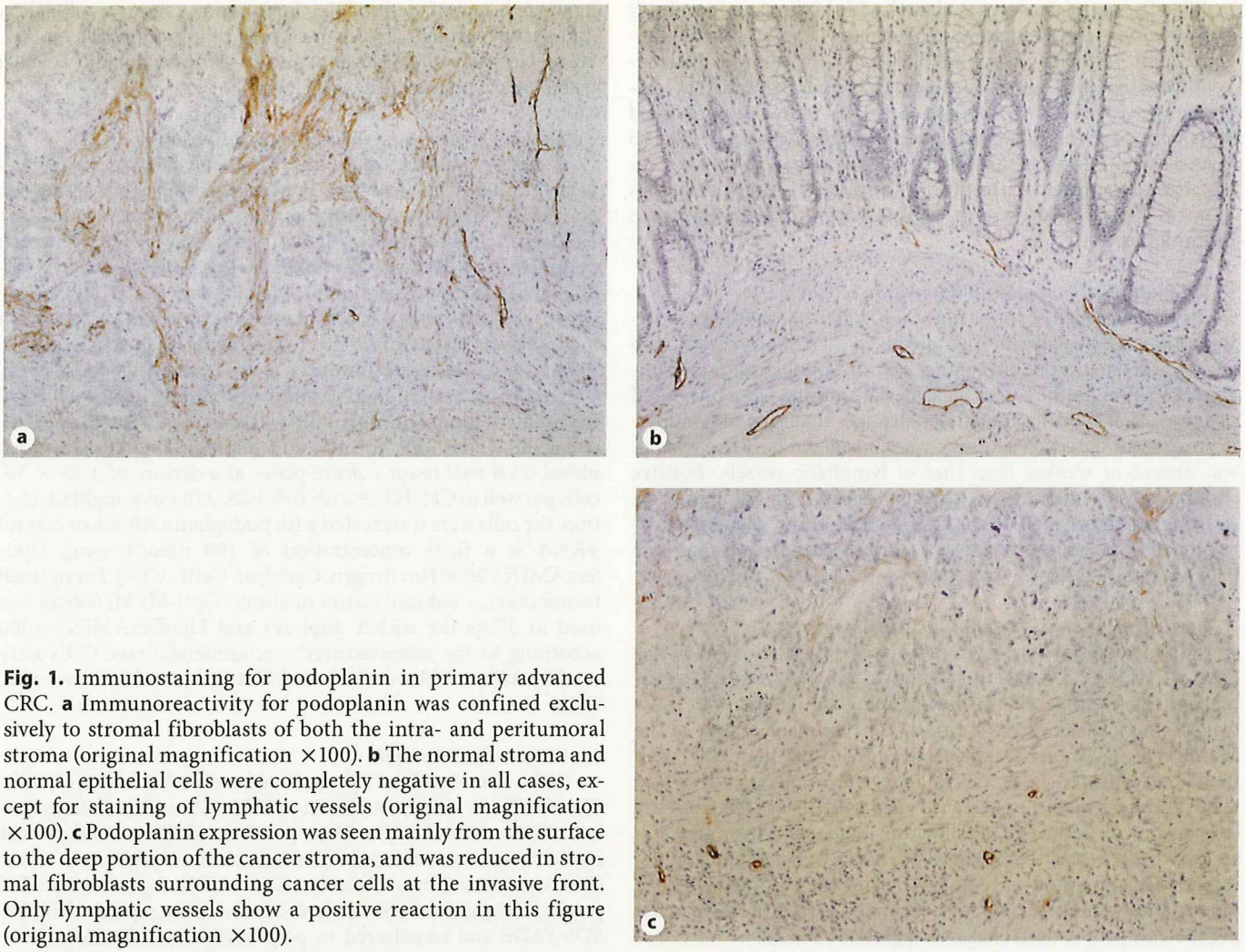

Fig. 1. Immunostaining for podoplanin in primary advanced CRC. **a** Immunoreactivity for podoplanin was confined exclusively to stromal fibroblasts of both the intra- and peritumoral stroma (original magnification ×100). **b** The normal stroma and normal epithelial cells were completely negative in all cases, except for staining of lymphatic vessels (original magnification ×100). **c** Podoplanin expression was seen mainly from the surface to the deep portion of the cancer stroma, and was reduced in stromal fibroblasts surrounding cancer cells at the invasive front. Only lymphatic vessels show a positive reaction in this figure (original magnification ×100).

HCT15 cells were seeded onto each of the upper chambers in CM-HT29 with 1% FBS at a density of 2×10^5 cells, where the fibroblasts were in a confluent state. Carcinoma cells were allowed to migrate through both the transfected fibroblasts and the Matrigel matrix membrane for 24 h at 37°C. After incubation, the nonmigrated cells in the upper chamber were gently removed with a cotton swab, and the carcinoma cells that had invaded through the Matrigel-coated inserts were stained with Diff-Quik (Sysmex, Kobe, Japan). The number of carcinoma cells on the lower side in 5 randomly chosen areas per membrane was counted under a light microscope at ×100 magnification. Means were based on the numbers obtained from the 5 randomly chosen areas for each treatment condition. All assays were performed in triplicate, and the differences in the counts of cells that had invaded among the carcinoma cells that had been cocultured with fibroblasts transfected with either podoplanin siRNA or control siRNA were analyzed using Student's t test. Statistical tests were two-sided at a 5% level of significance.

Results

Podoplanin Expression in CRC

Immunoreactivity for podoplanin was located in the cytoplasm and cell membrane of fibroblasts surrounding carcinoma cells. Immunoreactivity for podoplanin was confined exclusively to the stromal fibroblasts of both the intra- and the peritumoral stroma, and absent in stromal cells surrounding cancer cells budding from the tumor nests at the invasive front. Podoplanin expression was seen in stromal fibroblasts located mainly from the superficial to the deep area of the tumor, sparing the invasive front (fig. 1a–c), whereas normal stroma was completely negative in all cases except for lymphatic vessels (fig. 1). Podoplanin-positive staining was not observed in either normal epithelial cells or carcinoma cells. Fifty cases (41.7%) belonged to group A.

Table 1. Correlations between podoplanin expression and clinicopathological factors in patients with advanced CRC (stages II and III)

Variables	Podoplanin		p value
	group A (over 30)	group B (fewer than 30)	
Age, years	60.0 ± 11.7	61.3 ± 10.7	0.5105[1]
Gender			
Male	30 (25.0)	46 (38.3)	
Female	20 (16.7)	24 (20.0)	0.5219[2]
Tumor location			
Colon	23 (19.2)	48 (40.0)	
Rectum	27 (22.5)	22 (18.3)	0.0131[2]
Maximum diameter of the tumor			0.1565[3]
mm (median, range)	42, 15–107	49, 15–110	
Depth of invasion (pT)[4]			
T2	8 (6.7)	2 (1.7)	
T3	42 (35.0)	64 (53.3)	
T4	0	4 (3.3)	0.0106[2]
Lymph node metastasis (pN)			
Absence	25 (20.8)	25 (20.8)	
Presence	25 (20.8)	45 (37.5)	0.1176[2]
Histological grade[5]			
G1	19 (15.8)	22 (18.3)	
G2	30 (25.0)	45 (37.5)	
G3	1 (0.8)	3 (2.5)	0.634[2]
Lymphatic invasion			
Absence	12 (10.0)	13 (10.8)	
Presence	38 (31.7)	57 (47.5)	0.4704[2]
Venous invasion			
Absence	18 (15.0)	17 (14.2)	
Presence	32 (26.7)	53 (44.2)	0.164[2]

Figures in parentheses are percentages.
[1] Student's t test.
[2] χ^2 test or Fisher's exact test.
[3] Mann-Whitney U test.
[4] T2: tumor invades the muscularis propia; T3: tumor invades through the muscularis propia into the subserosa or peritoneal tissues; T4: tumor directly invades other organs or structures and/or perforates visceral peritoneum.
[5] G1: well-differentiated adenocarcinoma; G2: moderately differentiated adenocarcinoma; G3: poorly differentiated adenocarcinoma including signet ring cell adenocarcinoma and mucinous adenocarcinoma.

Prognostic Value of Podoplanin Expression in Patients with CRC

The correlations between podoplanin expression and clinicopathological factors are summarized in table 1. Group A was significantly correlated with a more distal tumor localization (p = 0.013) and a shallower depth of tumor invasion (p = 0.011) (table 1). There was no significant correlation between podoplanin expression, and age, gender, maximum tumor diameter, lymph node metastasis (pN), histological grade, lymphatic invasion, or venous invasion (table 1).

Patients in group A survived significantly longer than those who were negative, in terms of both disease-specific survival (DSS) and disease-free survival (DFS) (p = 0.0017 and p < 0.0001, respectively; fig. 2a, b). Patients in group A showed a significantly lower incidence of liver metastasis than patients in group B (p = 0.001; fig. 2c). For both DSS and DFS, univariate analysis using the Cox proportional hazards model revealed that podoplanin expression, depth of invasion (pT), and pN were significantly associated with prognosis (table 2), and that both podoplanin expression and pT were significantly associated with liver metastasis (table 2). Venous invasion factor tended to correlate with recurrence-free survival and liver metastasis-free survival (p = 0.086 and p = 0.051, respectively; table 2), but this tendency did not reach statistical significance. Multivariate analysis using the Cox proportional hazards model revealed that negative podoplanin expression and presence of pN were significantly associated with reduced DSS when adjusted for pT and venous invasion (p = 0.016 and p = 0.027, respectively; table 3). Multivariate analysis for both DFS and liver metastasis-free survival revealed that only podoplanin expression was associated with prognosis when adjusted for pT, pN, and venous invasion (p = 0.0023 and p = 0.020, respectively; table 3).

Results of Invasion Assay

To explore the biological role of podoplanin in fibroblasts, we used the RNA interference (RNAi) strategy to downregulate its expression. Increased podoplanin expression was observed in CAFs with CM-HT29, whereas it was not constitutively expressed in CCD112CoN cultured with low-serum medium. The podoplanin protein level in CAFs was substantially reduced within 72 h after transfection with 100 nmol/l podoplanin siRNA (fig. 3a). The result indicated that podoplanin siRNA effectively and specifically downregulated podoplanin protein expression in CAFs.

A tumor invasion assay was then performed using the Matrigel model to investigate whether reduced expression of podoplanin in CAFs increased the invasiveness of CRC cell lines in coculture. When CRC cell lines such as HCT116 and HCT15 were cocultured with CAFs transfected with control siRNA for podoplanin, a few invading cells were observed. However, when CRC cell lines were cocultured with CAFs transfected with siRNA1 for podo-

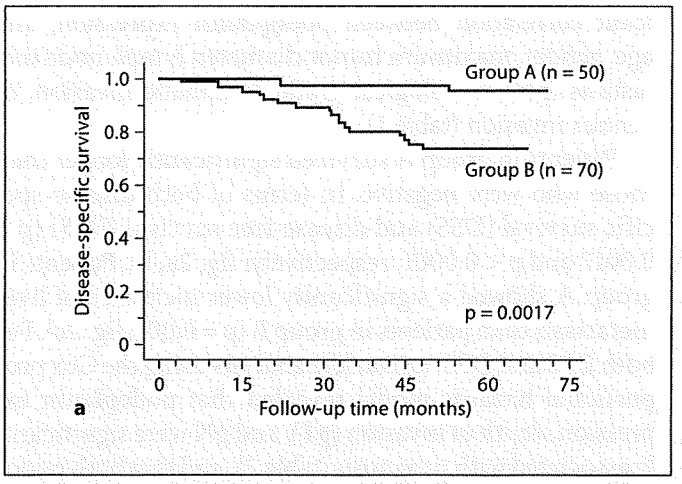

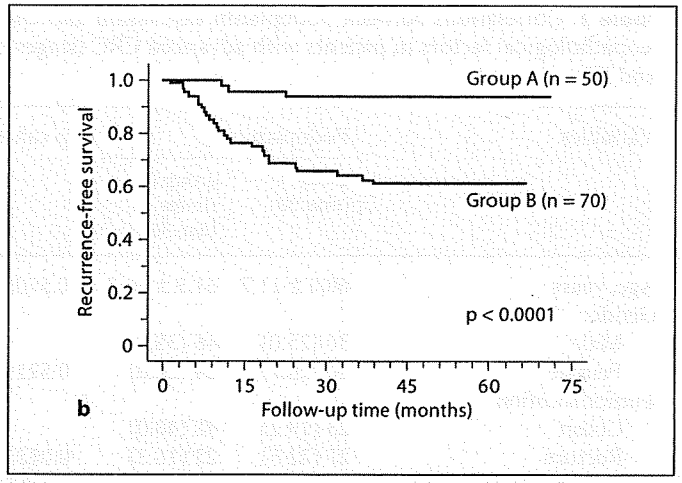

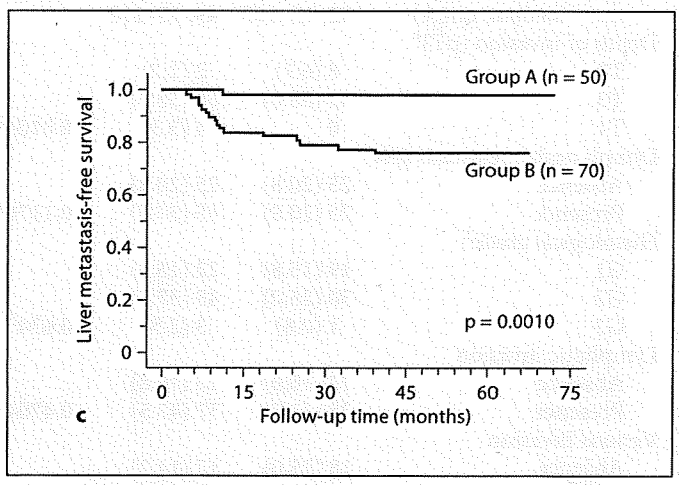

Fig. 2. Podoplanin expression and survival in 120 CRC cases at the National Cancer Center Research Hospital. DSS (**a**), DFS (**b**), and liver metastasis-free survival (**c**) of the patients in relation to podoplanin expression ($p = 0.0017$, $p < 0.0001$ and $p = 0.0010$, respectively).

Table 2. Univariate Cox proportional hazards analysis in patients with advanced CRC (stages II and III)

Prognostic factors	Disease-specific survival			Recurrence-free survival			Liver metastasis-free survival		
	HR	95% CI	p value	HR	95% CI	p value	HR	95% CI	p value
Expression of podoplanin (group A/group B)	0.135	0.031–0.586	0.0075	0.128	0.039–0.425	0.0008	0.075	0.010–0.563	0.0118
Age (≥60 years/<60 years)[1]	1.329	0.535–3.306	0.5401	0.711	0.342–1.479	0.3613	0.793	0.306–2.056	0.6328
Gender (male/female)	1.371	0.521–3.607	0.5231	0.847	0.404–1.773	0.6585	0.838	0.319–2.203	0.7205
Tumor location (colon/rectum)	1.210	0.476–3.074	0.6888	0.966	0.461–2.022	0.9259	1.652	0.582–4.690	0.3459
Maximum diameter of the tumor (≥45/<45 mm)[1]	0.703	0.283–1.747	0.4475	0.565	0.267–1.196	0.1353	0.836	0.322–2.166	0.7117
Depth of invasion (T2, T3/T4)	0.207	0.048–0.898	0.0354	0.180	0.054–0.599	0.0052	0.175	0.040–0.771	0.0212
Lymph node metastasis (absence/presence)	0.217	0.063–0.744	0.0151	0.390	0.166–0.913	0.0300	0.527	0.185–1.496	0.2285
Histological grade (G1/G2, G3)	0.634	0.228–1.761	0.3819	0.562	0.240–1.315	0.1836	1.278	0.486–3.357	0.6192
Lymphatic invasion (presence/absence)	1.087	0.361–3.277	0.8819	1.878	0.653–5.397	0.2421	2.189	0.500–9.574	0.2981
Venous invasion (presence/absence)	1.681	0.558–5.066	0.3561	2.325	0.887–6.097	0.0862	7.511	0.996–56.666	0.0505

HR = Hazard ratio; CI = confidence interval. [1] Two groups are divided by the median.

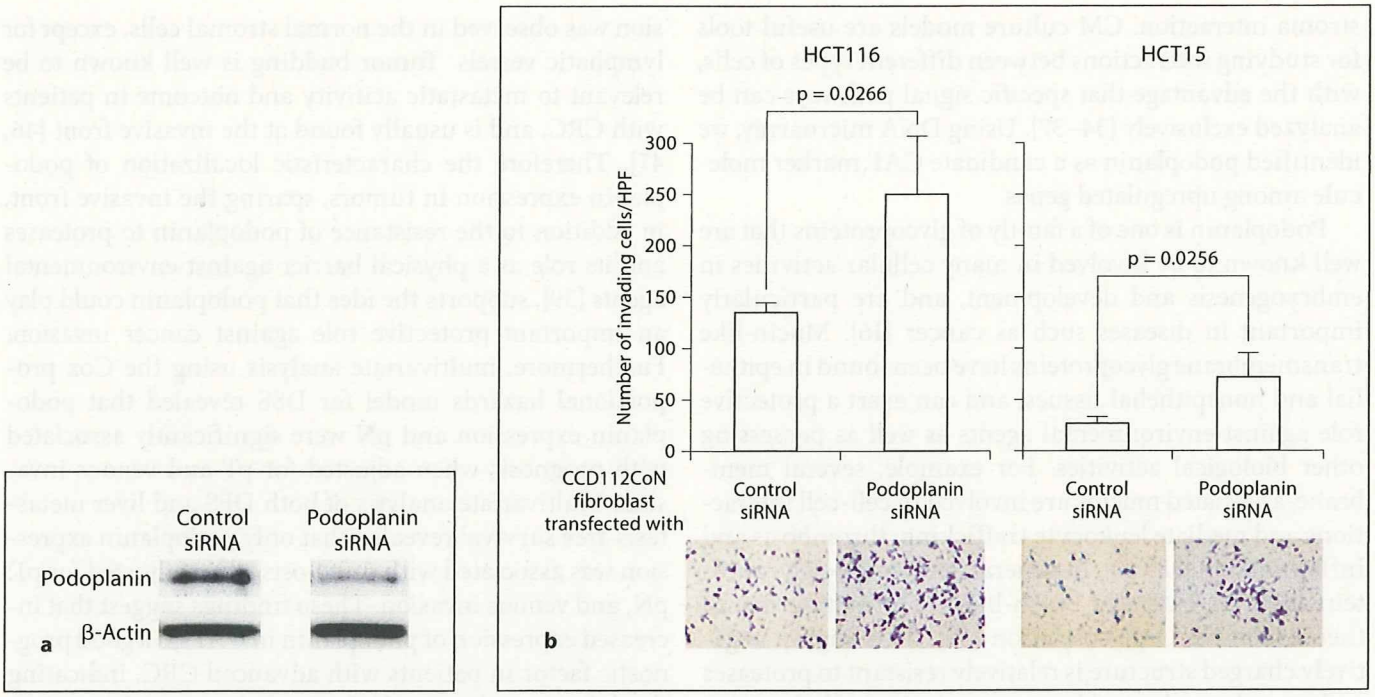

Fig. 3. Podoplanin expression in CCD112CoN fibroblast cells transfected with siRNAs and invasiveness of the cocultured CRC cell lines HCT116 and HCT15. **a** Western blotting using anti-D2–40 antibody (1:100; Dako) in the CCD112CoN fibroblast cells transfected with siRNAs. Podoplanin siRNA reduced podoplanin expression at the protein level almost completely. β-Actin was used as a loading control. **b** Invasiveness of HCT116 and HCT15 cells cocultured with fibroblasts transfected with podoplanin siRNA and control siRNA and in the Matrigel invasion system. After 24 h of coculture, CRC cell lines cocultured with fibroblasts transfected with podoplanin siRNA exhibited a 1.8- to 2.6-fold increase in the number of cells invading the Matrigel-coated insert. HPF = High-power field.

Table 3. Multivariate Cox proportional hazards analysis in patients with advanced CRC (stages II and III)

Prognostic factors	Disease-specific survival			Recurrence-free survival			Liver metastasis-free survival		
	HR	95% CI	p value	HR	95% CI	p value	HR	95% CI	p value
Expression of podoplanin (group A/group B)	0.161	0.037–0.708	0.0157	0.153	0.046–0.510	0.0023	0.089	0.012–0.682	0.0198
Depth of invasion (T2, T3/T4)	0.339	0.075–1.523	0.1582	0.308	0.089–1.066	0.0630	0.396	0.089–1.775	0.2264
Lymph node metastasis (absence/presence)	0.237	0.066–0.849	0.0270	0.488	0.201–1.184	0.1125	0.864	0.297–2.515	0.7888
Venous invasion (presence/absence)	0.858	0.269–2.739	0.7956	1.517	0.551–4.175	0.4194	5.745	0.727–45.380	0.0973

HR = Hazard ratio; CI = confidence interval.

planin, the number of invading cells was significantly increased ($p = 0.027$ and $p = 0.026$, Student's t test for coculture with HCT116 and HCT15, respectively; fig. 3b). As a negative control, when fibroblasts transfected with control siRNA and podoplanin siRNA were cultured only in CM-HT29 without CRC cell lines, almost no invading cells were evident (data not shown).

Discussion

To help understand the difference between CAFs and uninvolved fibroblasts, and to further evaluate the role of CAFs, we compared their genome-wide expression profiles using in vitro CM culture models in which soluble factors originating from cancer cells exerted a paracrine action on the surrounding fibroblasts involved in tumor-

stroma interaction. CM culture models are useful tools for studying interactions between different types of cells, with the advantage that specific signal pathways can be analyzed exclusively [34–37]. Using DNA microarray, we identified podoplanin as a candidate CAF marker molecule among upregulated genes.

Podoplanin is one of a family of glycoproteins that are well known to be involved in many cellular activities in embryogenesis and development, and are particularly important in diseases such as cancer [16]. Mucin-like transmembrane glycoproteins have been found in epithelial and nonepithelial tissues, and can exert a protective role against environmental agents as well as possessing other biological activities. For example, several membrane-associated mucins are involved in cell-cell interactions and mediate leukocyte trafficking, thrombosis and inflammation [38–40]. In general, mucin-type glycoproteins have an extended brush-like conformation due to their extensive O-glycosylation [39]. This highly negatively charged structure is relatively resistant to proteases and provides a physical barrier protecting cells from environmental agents.

In the present study, immunohistochemical localization of podoplanin was confined exclusively to CAFs in the cancer stroma. Normal stroma, epithelial cells and tumor cells were completely negative for podoplanin in all cases tested, and only lymphatic vessels were positive. Podoplanin expression in CAFs of cancer stroma was significantly correlated with more distal tumor localization and a shallower depth of tumor invasion. Invasion of CRC cell lines was augmented upon coculture with fibroblasts in which podoplanin expression was reduced by siRNA. These results indicate that podoplanin could play an important protective role against cancer invasion.

Expression of podoplanin by cancer cells of oral and uterine cervix squamous cell carcinoma has been reported to be associated with prognosis [41, 42]. However, previous studies have found that adenocarcinoma cells rarely express podoplanin [43, 44]. Podoplanin-positive CAFs are reportedly present in invasive adenocarcinoma of the lung, but not in noninvasive adenocarcinoma [45]. Podoplanin expression by CAFs is reported to be significantly associated with a poor outcome in patients with lung adenocarcinoma. However, multivariate analysis failed to show that podoplanin expression was an independent prognostic factor [45]. In the present study, the localization of podoplanin expression was intriguing because it was seen in CAFs located mainly in the superficial to deep area of the tumor, sparing the invasive front where tumor budding is often observed. No podoplanin expression was observed in the normal stromal cells, except for lymphatic vessels. Tumor budding is well known to be relevant to metastatic acitivity and outcome in patients with CRC, and is usually found at the invasive front [46, 47]. Therefore the characteristic localization of podoplanin expression in tumors, sparing the invasive front, in addition to the resistance of podoplanin to proteases and its role as a physical barrier against environmental agents [39], supports the idea that podoplanin could play an important protective role against cancer invasion. Furthermore, multivariate analysis using the Cox proportional hazards model for DSS revealed that podoplanin expression and pN were significantly associated with prognosis when adjusted for pT and venous invasion. Multivariate analysis of both DFS and liver metastasis-free survival revealed that only podoplanin expression was associated with prognosis when adjusted for pT, pN, and venous invasion. These findings suggest that increased expression of podoplanin in CAFs is a good prognostic factor in patients with advanced CRC, indicating the defensive role of podoplanin against tumor invasion. In terms of clinical use, podoplanin expression in CRC might be helpful for selecting patients who should undergo adjuvant chemotherapy, or those for whom it is unnecessary. However, in order for podoplanin expression to be applied for practical clinical care, it must be validated in a large-scale prospective clinical trial.

Furthermore, our coculture invasion assay indicated that podoplanin expressed in CAFs could have a suppressive effect on the invasion of tumor cells, although it is not yet clear whether CAFs have both an inductive and a suppressive effect on tumor progression and regulate tumorigenesis. Other constituents of the desmoplastic extracellular matrix have also been shown to inhibit tumor progression. For example, injection of L-3, 4-dehydroproline, which inhibits the formation of collagen fibrils, increases tumor cell invasion in mice with B16F10 melanoma subcutaneous tumors [48]. In addition, extracellular matrix accumulation in tumors contributes to increased interstitial fluid pressure and hinders the diffusion of macromolecules and oxygen, leading to tumor cell necrosis [49, 50]. The overall effect of altered extracellular matrix in tumors and the effect of CAFs during tumor progression are still poorly understood. Further studies directed at disrupting the complex interaction between tumor cells and stromal composition may define new strategies for diagnosis of tumors and suitable therapeutic interventions.

In conclusion, podoplanin, a mucin-type transmembrane glycoprotein, was found to be upregulated in CAFs

in vitro and to be overexpressed in CAFs surrounding CRC cells in vivo. Multivariate analysis of both DFS and liver metastasis-free survival revealed that only podoplanin expression was associated with prognosis when adjusted for pT, pN, and venous invasion. In addition, invasiveness of CRC cells was increased significantly by coculture with podoplanin-suppressed CAFs. These findings suggest that increased podoplanin expression in stromal fibroblasts is a significant indicator of good prognosis in patients with advanced CRC, reflecting its defensive role against cancer invasion.

Acknowledgement

This study was supported by a grant-in-aid for the Third Term Comprehensive 10-Year Strategy for Cancer Control from the Ministry of Health, Labor and Welfare of Japan. T. Y. is a recipient of a Research Resident Fellowship from the Foundation for Promotion of Cancer Research in Japan.

References

1 Bhowmick NA, Neilson EG, Moses HL: Stromal fibroblasts in cancer initiation and progression. Nature 2004;432:332–337.
2 De Wever O, Mareel M: Role of tissue stroma in cancer cell invasion. J Pathol 2003;200:429–447.
3 Kalluri R, Zeisberg M: Fibroblasts in cancer. Nat Rev Cancer 2006;6:392–401.
4 Micke P, Ostman A: Exploring the tumour environment: cancer-associated fibroblasts as targets in cancer therapy. Expert Opin Ther Targets 2005;9:1217–1233.
5 Bhowmick NA, Chytil A, Plieth D, et al: TGF-β signaling in fibroblasts modulates the oncogenic potential of adjacent epithelia. Science 2004;303:848–851.
6 Orimo A, Gupta PB, Sgroi DC, et al: Stromal fibroblasts present in invasive human breast carcinomas promote tumor growth and angiogenesis through elevated SDF-1/CXCL12 secretion. Cell 2005;121:335–348.
7 Olumi AF, Grossfeld GD, Hayward SW, Carroll PR, Tlsty TD, Cunha GR: Carcinoma-associated fibroblasts direct tumor progression of initiated human prostatic epithelium. Cancer Res 1999;59:5002–5011.
8 Dimanche-Boitrel MT, Vakaet L Jr, Pujuguet P, et al: In vivo and in vitro invasiveness of a rat colon-cancer cell line maintaining E-cadherin expression: an enhancing role of tumor-associated myofibroblasts. Int J Cancer 1994;56:512–521.
9 Sternlicht MD, Lochter A, Sympson CJ, et al: The stromal proteinase MMP3/stromelysin-1 promotes mammary carcinogenesis. Cell 1999;98:137–146.
10 Lochter A, Galosy S, Muschler J, Freedman N, Werb Z, Bissell MJ: Matrix metalloproteinase stromelysin-1 triggers a cascade of molecular alterations that leads to stable epithelial-to-mesenchymal conversion and a premalignant phenotype in mammary epithelial cells. J Cell Biol 1997;139:1861–1872.
11 Cornil I, Theodorescu D, Man S, Herlyn M, Jambrosic J, Kerbel RS: Fibroblast cell interactions with human melanoma cells affect tumor cell growth as a function of tumor progression. Proc Natl Acad Sci USA 1991;88:6028–6032.
12 Mishima K, Kato Y, Kaneko MK, Nishikawa R, Hirose T, Matsutani M: Increased expression of podoplanin in malignant astrocytic tumors as a novel molecular marker of malignant progression. Acta Neuropathol (Berl) 2006;111:483–488.
13 Yuan P, Temam S, El-Naggar A, et al: Overexpression of podoplanin in oral cancer and its association with poor clinical outcome. Cancer 2006;107:563–569.
14 Schacht V, Dadras SS, Johnson LA, Jackson DG, Hong YK, Detmar M: Up-regulation of the lymphatic marker podoplanin, a mucin-type transmembrane glycoprotein, in human squamous cell carcinomas and germ cell tumors. Am J Pathol 2005;166:913–921.
15 Zimmer G, Oeffner F, Von Messling V, et al: Cloning and characterization of gp36, a human mucin-type glycoprotein preferentially expressed in vascular endothelium. Biochem J 1999;341:277–284.
16 Brockhausen I, Schutzbach J, Kuhns W: Glycoproteins and their relationship to human disease. Acta Anat (Basel) 1998;161:36–78.
17 Martin-Villar E, Scholl FG, Gamallo C, et al: Characterization of human PA2.26 antigen (T1α-2, podoplanin), a small membrane mucin induced in oral squamous cell carcinomas. Int J Cancer 2005;113:899–910.
18 Ordonez NG: Podoplanin: a novel diagnostic immunohistochemical marker. Adv Anat Pathol 2006;13:83–88.
19 Breiteneder-Geleff S, Soleiman A, Kowalski H, et al: Angiosarcomas express mixed endothelial phenotypes of blood and lymphatic capillaries: podoplanin as a specific marker for lymphatic endothelium. Am J Pathol 1999;154:385–394.
20 Schacht V, Ramirez MI, Hong YK, et al: T1α/podoplanin deficiency disrupts normal lymphatic vasculature formation and causes lymphedema. Embo J 2003;22:3546–3556.
21 Wicki A, Lehembre F, Wick N, Hantusch B, Kerjaschki D, Christofori G: Tumor invasion in the absence of epithelial-mesenchymal transition: podoplanin-mediated remodeling of the actin cytoskeleton. Cancer Cell 2006;9:261–272.
22 Sugimoto Y, Watanabe M, Oh-hara T, Sato S, Isoe T, Tsuruo T: Suppression of experimental lung colonization of a metastatic variant of murine colon adenocarcinoma 26 by a monoclonal antibody 8F11 inhibiting tumor cell-induced platelet aggregation. Cancer Res 1991;51:921–925.
23 Watanabe M, Okochi E, Sugimoto Y, Tsuruo T: Identification of a platelet-aggregating factor of murine colon adenocarcinoma as determined by monoclonal antibodies. Cancer Res 1988;48:6411–6416.
24 Kato Y, Kaneko M, Sata M, Fujita N, Tsuruo T, Osawa M: Enhanced expression of Aggrus (T1α/podoplanin), a platelet-aggregation-inducing factor in lung squamous cell carcinoma. Tumour Biol 2005;26:195–200.
25 Kimura N, Kimura I: Podoplanin as a marker for mesothelioma. Pathol Int 2005;55:83–86.
26 Ordonez NG: D2–40 and podoplanin are highly specific and sensitive immunohistochemical markers of epithelioid malignant mesothelioma. Hum Pathol 2005;36:372–380.
27 Roy S, Chu A, Trojanowski JQ, Zhang PJ: D2–40, a novel monoclonal antibody against the M2A antigen as a marker to distinguish hemangioblastomas from renal cell carcinomas. Acta Neuropathol (Berl) 2005;109:497–502.

28 Kato Y, Sasagawa I, Kaneko M, Osawa M, Fujita N, Tsuruo T: Aggrus: a diagnostic marker that distinguishes seminoma from embryonal carcinoma in testicular germ cell tumors. Oncogene 2004;23:8552–8556.
29 Shibahara J, Kashima T, Kikuchi Y, Kunita A, Fukayama M: Podoplanin is expressed in subsets of tumors of the central nervous system. Virchows Arch 2006;448:493–499.
30 Mishima K, Kato Y, Kaneko MK, et al: Podoplanin expression in primary central nervous system germ cell tumors: a useful histological marker for the diagnosis of germinoma. Acta Neuropathol (Berl) 2006;111:563–568.
31 Gandarillas A, Scholl FG, Benito N, Gamallo C, Quintanilla M: Induction of PA2.26, a cell-surface antigen expressed by active fibroblasts, in mouse epidermal keratinocytes during carcinogenesis. Mol Carcinog 1997;20:10–18.
32 Sobin LH, Fleming ID: TNM Classification of Malignant Tumors, ed 5 (1997). Union Internationale contre le Cancer and the American Joint Committee on Cancer. Cancer 1997;80:1803–1804.
33 World Health Organization: Classification of Tumours. Lyon, IARC Press, 2000.
34 DeCosse JJ, Gossens C, Kuzma JF, Unsworth BR: Embryonic inductive tissues that cause histologic differentiation of murine mammary carcinoma in vitro. J Natl Cancer Inst 1975;54:913–922.
35 DeCosse JJ, Gossens CL, Kuzma JF, Unsworth BR: Breast cancer: induction of differentiation by embryonic tissue. Science 1973;181:1057–1058.
36 Cooper M, Pinkus H: Intrauterine transplantation of rat basal cell carcinoma as a model for reconversion of malignant to benign growth. Cancer Res 1977;37:2544–2552.
37 Maehara N, Matsumoto K, Kuba K, Mizumoto K, Tanaka M, Nakamura T: NK4, a four-kringle antagonist of HGF, inhibits spreading and invasion of human pancreatic cancer cells. Br J Cancer 2001;84:864–873.
38 Gendler SJ, Spicer AP: Epithelial mucin genes. Annu Rev Physiol 1995;57:607–634.
39 Hilkens J, Ligtenberg MJ, Vos HL, Litvinov SV: Cell membrane-associated mucins and their adhesion-modulating property. Trends Biochem Sci 1992;17:359–363.
40 Varki A: Selectin ligands. Proc Natl Acad Sci USA 1994;91:7390–7397.
41 Yuan P, Temam S, El-Naggar A, Zhou X, Liu DD, Lee JJ, Mao L: Overexpression of podoplanin in oral cancer and its association with poor clinical outcome. Cancer 2006;107:563–569.
42 Dumoff KL, Chu CS, Harris EE, Holtz D, Xu X, Zhang PJ, ACS G: Low podoplanin expression in pretreatment biopsy material predicts poor prognosis in advanced-stage squamous cell carcinoma of the uterine cervix treated by primary radiation. Mod Pathol 2006;19:708–716.
43 Ordonez NG: D2–40 and podoplanin are highly specific and sensitive immunohistochemical markers of epithelioid malignant mesothelioma. Hum Pathol 2005;36:372–380.
44 Chu AY, Litzky LA, Pasha TL, Acs G, Zhang PJ: Utility of D2–40, a novel mesothelial marker, in the diagnosis of malignant mesothelioma. Mod Pathol 2005;18:105–110.
45 Kawase A, Ishii G, Nagai K, Ito T, Nagano T, Murata Y, Hishida T, Nishimura M, Yoshida J, Suzuki K, Ochiai A: Podoplanin expression by cancer associated fibroblasts predicts poor prognosis of lung adenocarcinoma. Int J Cancer 2008;123:1053–1059.
46 Okuyama T, Oya M, Ishikawa H: Budding as a risk factor for lymph node metastasis in pT1 or pT2 well-differentiated colorectal adenocarcinoma. Dis Colon Rectum 2002;45:628–634.
47 Ueno H, Price AB, Wilkinson KH, Jass JR, Mochizuki H, Talbot IC: A new prognostic staging system for rectal cancer. Ann Surg 2004;240:832–839.
48 Barsky SH, Gopalakrishna R: Increased invasion and spontaneous metastasis of BL6 melanoma with inhibition of the desmoplastic response in C57 BL/6 mice. Cancer Res 1987;47:1663–1667.
49 Netti PA, Berk DA, Swartz MA, Grodzinsky AJ, Jain RK: Role of extracellular matrix assembly in interstitial transport in solid tumors. Cancer Res 2000;60:2497–2503.
50 Brown EB, Boucher Y, Nasser S, Jain RK: Measurement of macromolecular diffusion coefficients in human tumors. Microvasc Res 2004;67:231–236.

Oncogene (2009) 28, 2738–2744

www.nature.com/onc

ORIGINAL ARTICLE

Chromatin remodeling at Alu repeats by epigenetic treatment activates silenced *microRNA-512-5p* with downregulation of *Mcl-1* in human gastric cancer cells

Y Saito[1], H Suzuki[1], H Tsugawa[1], I Nakagawa[1], J Matsuzaki[1], Y Kanai[2] and T Hibi[1]

[1]*Division of Gastroenterology and Hepatology, Department of Internal Medicine, Keio University School of Medicine, Shinjuku-ku, Tokyo, Japan and* [2]*Pathology Division, National Cancer Center Research Institute, Chuo-ku, Tokyo, Japan*

Epigenetic therapy using DNA methylation inhibitors and histone deacetylase (HDAC) inhibitors has clinical promise for the treatment of human malignancies. To investigate roles of microRNAs (miRNAs) on epigenetic therapy of gastric cancer, the miRNA expression profile was analysed in human gastric cancer cells treated with 5-aza-2′-deoxycytidine (5-Aza-CdR) and 4-phenylbutyric acid (PBA). miRNA microarray analysis shows that most of miRNAs activated by 5-Aza-CdR and PBA in gastric cancer cells are located at Alu repeats on chromosome 19. Analyses of chromatin modification show that DNA demethylation and HDAC inhibition at Alu repeats activates silenced *miR-512-5p* by RNA polymerase II. In addition, activation of *miR-512-5p* by epigenetic treatment induces suppression of *Mcl-1*, resulting in apoptosis of gastric cancer cells. These results suggest that chromatin remodeling at Alu repeats plays critical roles in the regulation of miRNA expression and that epigenetic activation of silenced Alu-associated miRNAs could be a novel therapeutic approach for gastric cancer.
Oncogene (2009) **28**, 2738–2744; doi:10.1038/onc.2009.140; published online 8 June 2009

Keywords: miRNA; DNA methylation; histone modification; epigenetic treatment; Alu repeats; gastric cancer

Introduction

Chromatin-modifying drugs such as DNA methylation inhibitors and histone deacetylase (HDAC) inhibitors are emerging as effective agents for 'epigenetic therapy' of cancer (Yoo and Jones, 2006; Gal-Yam *et al.*, 2008). In fact, the DNA methylation inhibitors 5-aza-2′-deoxycytidine (5-Aza-CdR) and 5-azacytidine (5-Aza-CR) were recently approved by the Food and Drug Administration for the treatment of myelodysplastic syndrome, and many HDAC inhibitors such as 4-phenylbutyric acid (PBA) are under clinical trials (Yoo and Jones, 2006). However, the molecular mechanisms underlying anticancer effect of these drugs are not fully understood.

MicroRNAs (miRNAs) are small non-coding RNAs, which can downregulate various target genes. miRNAs are expressed in a tissue-specific manner and have important functions in cellular proliferation, apoptosis and differentiation. Recent studies have indicated that aberrant expression of miRNAs contributes to the initiation and progression of human malignancies (Calin and Croce, 2006a, b). We have recently shown that some miRNAs are located near CpG islands and that expression of these miRNAs is regulated by alterations in DNA methylation and histone modification on their CpG islands (Saito and Jones, 2006; Saito *et al.*, 2006).

As the stomach is an organ in which epigenetic alterations due to *Helicobacter pylori* infection or various exogenous antigen exposures are frequently observed (Esteller, 2002), we are prompted to investigate miRNA expression profile in gastric cancer cells with epigenetic treatment. Interestingly, microarray analysis of AGS gastric cancer cells shows that most of the miRNAs, which are dramatically activated by 5-Aza-CdR and PBA, are located at Alu repeats on chromosome 19. Alu elements are ~280 bp in length and consist of two similar, but distinct, monomers linked by an oligo (dA) tract. It has been reported that Alu repeats in the miRNA cluster on chromosome 19 can function as RNA polymerase III (Pol III) promoters of miRNAs (Borchert *et al.*, 2006). Here we show that chromatin remodeling at Alu repeats by DNA demethylation and HDAC inhibition can activate expression of Alu-associated miRNAs, which can downregulate target oncogenes in human gastric cancer cells.

Results

miRNAs activated by epigenetic treatment in gastric cancer cells are located at Alu repeats on chromosome 19

To identify miRNAs, which are regulated by DNA demethylation and HDAC inhibition, we carried out miRNA microarray analysis. The miRNA expression profile of AGS human gastric cancer cells showed that 115 out of 470 miRNAs were differentially expressed by the treatment with 5-Aza-CdR and PBA ($P<0.01$).

Correspondence: Dr H Suzuki, Division of Gastroenterology and Hepatology, Department of Internal Medicine, Keio University School of Medicine, 35 Shinanomachi, Shinjuku-ku, Tokyo 160-8582, Japan. E-mail: hsuzuki@sc.itc.keio.ac.jp
Received 11 December 2008; revised 23 March 2009; accepted 18 April 2009; published online 8 June 2009

Interestingly, 14 out of top 15 miRNAs (93%) upregulated by epigenetic treatment are located in the miRNA cluster on chromosome 19 (Figure 1a) (Bentwich *et al.*, 2005). These miRNAs are interspersed among Alu repeats which can function as their promoters (Borchert *et al.*, 2006). We have recently reported that epigenetic treatment of T24 bladder cancer cells induced activation of only 5 Alu-associated miRNAs in top 15 miRNAs (33%) (Figure 1a) (Saito *et al.*, 2006). In addition, the signal ratios of Alu-associated miRNAs after epigenetic treatment in AGS cells compared with untreated cells were much higher than those in T24 cells. Therefore, activation of Alu-associated miRNAs by DNA demethylation and HDAC inhibition seems to be more specific in gastric cancer cells compared with bladder cancer cells.

To confirm the miRNA microarray data, we carried out quantitative reverse transcriptase (RT)–PCR analyses for *miR-512-5p, -517b, -526b, -518b* and *-515-5p* in AGS cells treated with 5-Aza-CdR and PBA. As shown in Figure 1b, all miRNAs examined were silenced before treatment and dramatically activated by 5-Aza-CdR and PBA treatment, which is consistent with the microarray data. Other gastric cancer cell lines (TMK1 and MKN45) also showed marked upregulation of *miR-512-5p* and *miR-517b* by epigenetic treatment (Figure 1c).

DNA demethylation and HDAC inhibition at Alu repeats activates silenced miR-512-5p

As epigenetic treatment remarkably upregulate expression of Alu-associated miRNAs, we examined DNA methylation and histone modification at the Alu promoter region of *miR-512* by bisulfite genomic sequencing and chromatin immunoprecipitation (ChIP) assay, respectively (Figures 2a and b). It was found that although the Alu promoter regions of *miR-512* were completely methylated (100%) in untreated AGS cells, DNA methylation levels were reduced to 20% after epigenetic treatment (Figure 2a).

Both acetylated histone H3 and methylated histone H3-lysine 4 (K4) are associated with an open chromatin structure and active gene expression. Significant increases in the levels of both acetylated histone H3 and methylated histone H3-K4 were found at the Alu promoter region of *miR-512* in AGS cells treated with 5-Aza-CdR and PBA (Figure 2b). These findings indicate that dense DNA methylation and closed chromatin structure at Alu repeats are associated with a silent state of *miR-512-5p*, and that chromatin remodeling at Alu repeats by DNA demethylation and HDAC inhibition activate silenced *miR-512-5p*.

a

AGS

No.	microRNA	Ratio	Locus	Alu
1	miR-512-5p	136	19q13	
2	miR-517b	84	19q13	
3	miR-517a	79	19q13	
4	miR-526b	42	19q13	
5	miR-518b	55	19q13	
6	miR-515-5p	45	19q13	
7	miR-512-3p	50	19q13	
8	miR-516-5p	50	19q13	
9	miR-520h	29	19q13	
10	miR-524*	26	19q13	
11	miR-127	23	14q32	
12	miR-520g	23	19q13	
13	miR-526a	22	19q13	
14	miR-520a*	21	19q13	
15	miR-525	20	19q13	

T24

No.	microRNA	Ratio	Locus	Alu
1	miR-127	49	14q32	
2	miR-377	44	14q32	
3	miR-494	36	14q32	
4	miR-495	31	14q32	
5	miR-517a	27	19q13	
6	miR-516-5p	26	19q13	
7	miR-517b	10	19q13	
8	miR-512-3p	8	19q13	
9	miR-192	6	11q13	
10	miR-193b	6	16p13	
11	miR-134	4	14q32	
12	miR-182	4	7q32	
13	miR-368	4	14q32	
14	miR-498	4	19q13	
15	miR-126	3	9q34	

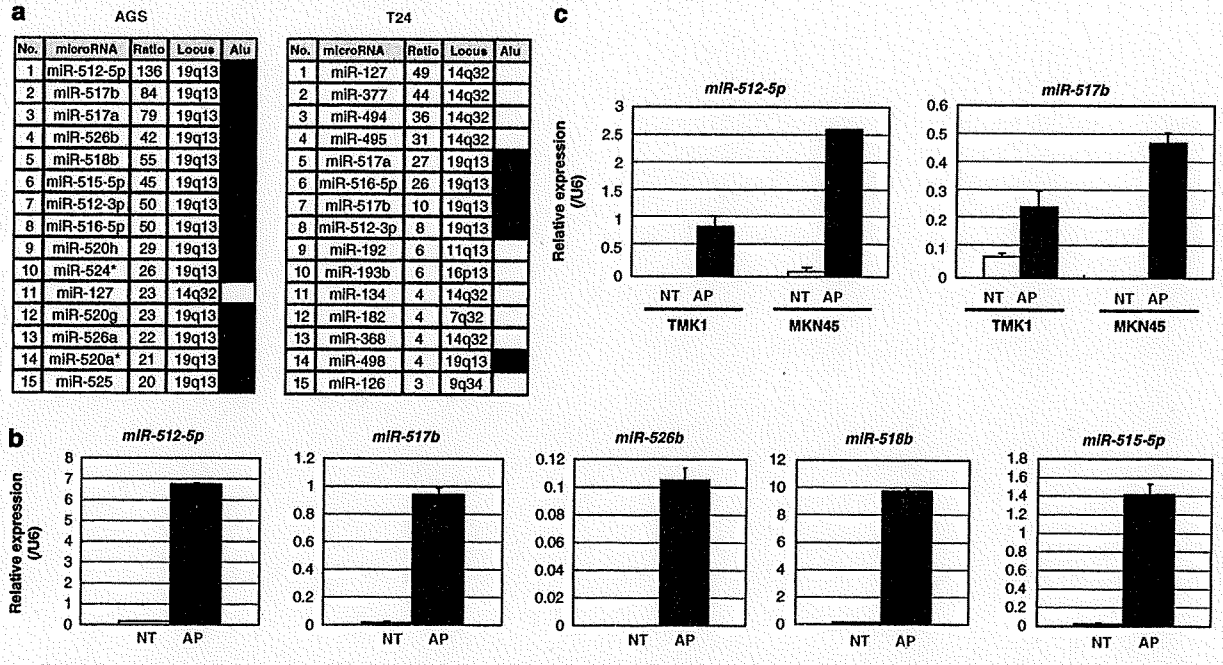

Figure 1 Expression patterns of Alu-associated microRNAs (miRNAs) in human gastric cancer cells treated with 5-aza-2′-deoxycytidine (5-Aza-CdR) and 4-phenylbutyric acid (PBA). (**a**) miRNAs upregulated by 5-Aza-CdR and PBA in AGS and T24 cells (microarray analysis). Ratio represents signal ratio of 5-Aza-CdR and PBA treatment compared with no treatment. Presence of Alu repeats in the upstream region of each miRNA is indicated by filled box. The expression profile of T24 is modified from Figure 1a of the reference (Saito *et al.*, 2006). (**b**) Quantitative reverse transcriptase (RT)–PCR analyses of Alu-associated miRNAs in AGS cells not treated (NT, blank bar) or treated with 5-Aza-CdR and PBA (AP, filled bar). The expression level was normalized to the U6 RNA expression level and expressed as mean + s.d. (**c**) Quantitative RT–PCR analyses of *miR-512-5p* and *miR-517b* in TMK1 and MKN45 cells not treated (NT, blank bar) or treated with 5-Aza-CdR and PBA (AP, filled bar). The expression level was normalized to the U6 RNA expression level and expressed as mean + s.d.

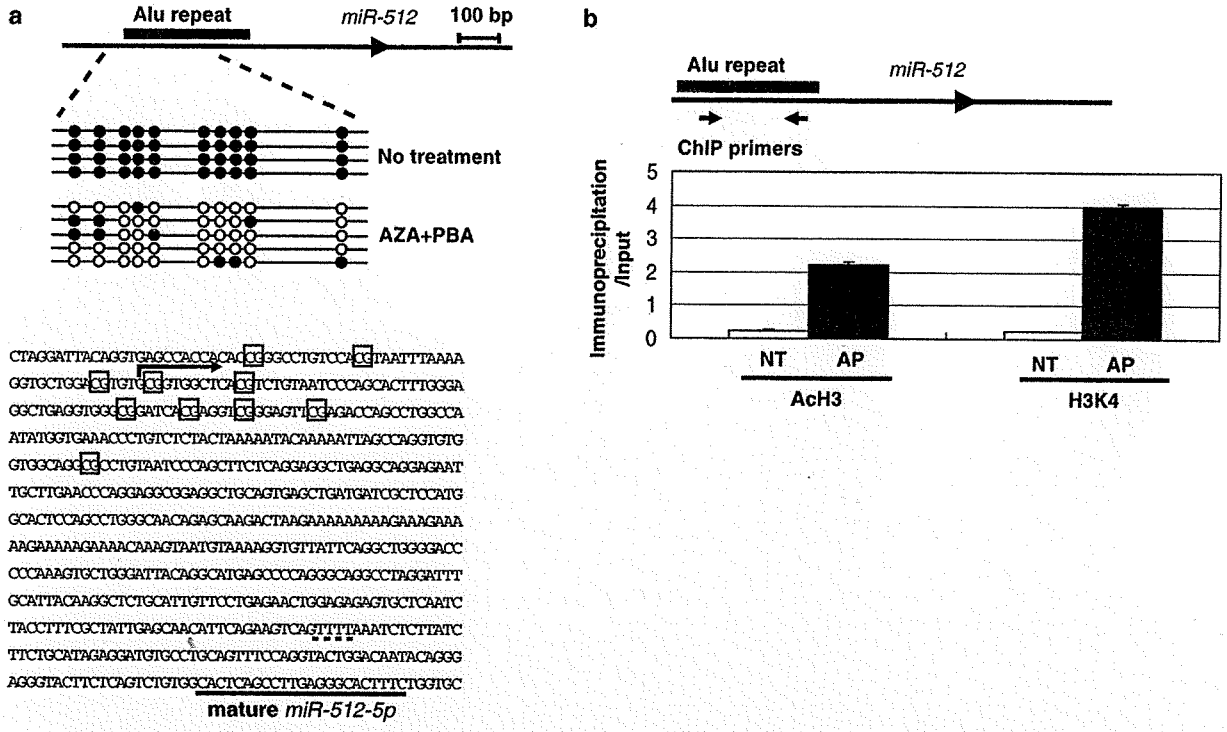

Figure 2 Alterations in DNA methylation and histone modification at Alu repeats of *miR-512* in AGS cells after epigenetic treatment. (**a**) DNA methylation status of CpG sites (shown as boxes) around the promoter region of *miR-512-5p* in AGS cells not treated or treated with 5-aza-2′-deoxycytidine (5-Aza-CdR) and 4-phenylbutyric acid (PBA) was determined by bisulfite genomic sequencing. Blank circle, unmethylated CpG; filled circle, methylated CpG. The bent arrow indicates the putative transcriptional start site of *miR-512-5p* determined by 5′ RACE assay. Note that Alu elements are separated from mature *miR-512-5p* sequences by Pol III terminator (TTTT, dot line), indicating that Pol III at Alu elements cannot transcribe *miR-512-5p*. (**b**) The levels of acetylated histone H3 (AcH3) and dimethylated histone H3-K4 (H3K4) of *miR-512-5p* were determined by chromatin immunoprecipitation (ChIP) assay in AGS cells not treated (NT, blank bar) or treated with 5-Aza-CdR and PBA (AP, filled bar). Immunoprecipitation/Input = (immunoprecipitated DNA with each antibody −No Antibody Control (NAC))/(input DNA−NAC). Values are expressed as mean + s.d.

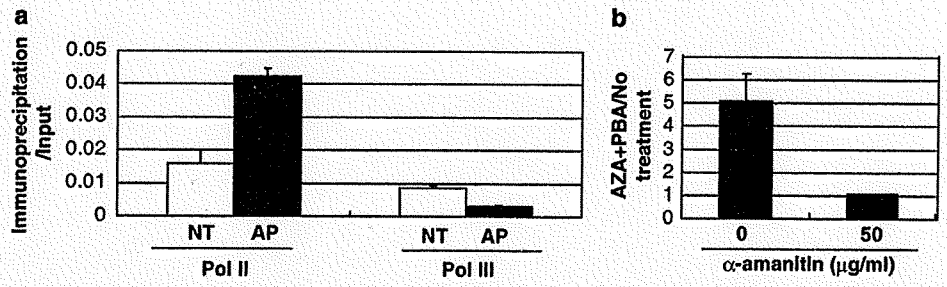

Figure 3 Activation of *miR-512-5p* by epigenetic treatment is mediated by Pol II. (**a**) Levels of Pol II and Pol III around the promoter regions of *miR-512-5p* were determined by chromatin immunoprecipitation assay in AGS cells not treated (NT, blank bar) or treated with 5-aza-2′-deoxycytidine (5-Aza-CdR) and 4-phenylbutyric acid (PBA) (AP, filled bar). Immunoprecipitation/Input = (immunoprecipitated DNA with each antibody −No Antibody Control (NAC))/(input DNA−NAC). Values are expressed as mean + s.d. (**b**) AGS cells treated with 5-Aza-CdR and PBA were incubated in 0 or 50 μg/ml of α-amanitin for 7 h before the cells were harvested for assay. Ratios of 5-Aza-CdR and PBA treatment compared with no treatment in expression levels of *miR-512-5p* normalized with U6 were shown. Values are expressed as mean + s.d.

Activation of miR-512-5p *by epigenetic treatment is mediated by Pol II*

To assess whether epigenetic activation of *miR-512-5p* is mediated by Pol II or Pol III, we have carried out ChIP assay of Pol II and Pol III on the promoter region of *miR-512-5p* in AGS cells (Figure 3a). The results of ChIP assay show that Pol II signal at Alu repeats is significantly increased after epigenetic treatment, whereas Pol III signal shows no increase. Pol II is highly sensitive to α-amanitin and therefore treatment of

mammalian cells with α-amanitin at a concentration of 50 μg/ml for 5–9 h results in the selective inhibition of Pol II. AGS cells with epigenetic treatment were incubated in 0 or 50 μg/ml of α-amanitin for 7 h before the cells were harvested for assay. As shown in Figure 3b, we have found that the epigenetic activation of *miR-512-5p* is inhibited by α-amanitin treatment. In addition, we have identified the putative Pol II transcriptional start site of *miR-512-5p* by 5′-rapid amplification of cDNA ends (5′-RACE) (Figure 2a). These findings indicate that activation of *miR-512-5p* by epigenetic treatment is mediated by Pol II.

Overexpression of miR-512-5p *suppresses* Mcl-1 *and induces apoptosis*

Identification of target genes of Alu-associated miRNAs is essential to investigate their biological function. Recent studies have shown that miRNAs can regulate expression of their target genes by decreasing mRNA stability, in addition to translational inhibition (Yekta *et al*., 2004; Bagga *et al*., 2005; Wu *et al*., 2006). The strategy to identify target genes of *miR-512-5p* is shown in Figure 4a. First of all, we conducted a microarray analysis to screen for genes that were threefold downregulated by treatment with 5-Aza-CdR and PBA, because target genes of *miR-512-5p* were expected to be suppressed by overexpression of *miR-512-5p*. Then, we identified 69 genes, which are known to be involved in cell proliferation, apoptosis and differentiation. We finally selected nine genes as potential target genes of *miR-512-5p* by referring to the database for the prediction of miRNA targets (microRNA.org, http://www.microrna.org). Among these nine genes, we especially focused on well-known oncogenes, *Jun* and *Mcl-1*. To confirm that *Jun* and *Mcl-1* are target genes of *miR-512-5p*, AGS cells were transfected with *miR-512-5p* precursor molecules, and the expression levels of *Jun* and *Mcl-1* were assessed by quantitative RT–PCR. As shown in Figure 4b, significant downregulation of *Jun* and *Mcl-1* was observed in AGS cells after transfection of *miR-512-5p*. As the expression of *Mcl-1* was remarkably downregulated by overexpression of *miR-512-5p*, we further examined expression level of Mcl-1 by western blotting. The expression level of Mcl-1 was significantly downregulated in AGS cells both after

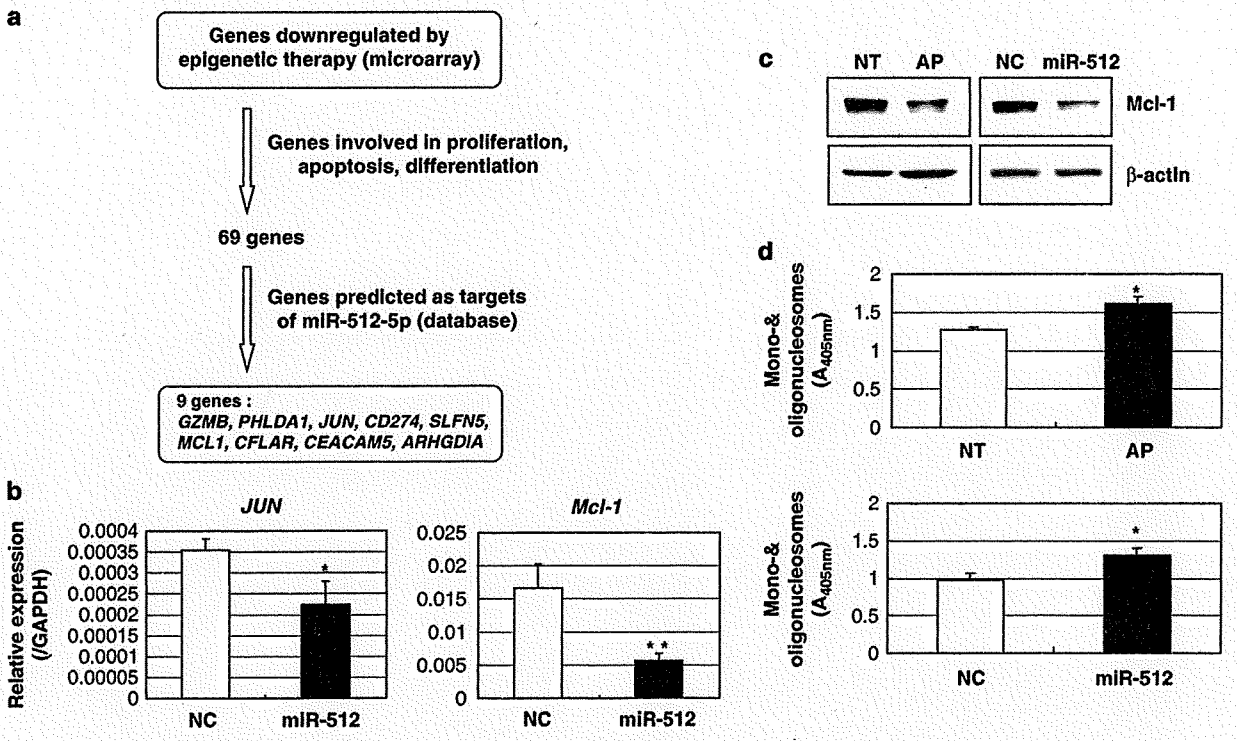

Figure 4 Overexpression of *miR-512-5p* induces suppression of *Mcl-1* and apoptosis. (**a**) A schema to identify targets of *miR-512-5p* using the microarray data of AGS cells treated with 5-aza-2′-deoxycytidine (5-Aza-CdR) and 4-phenylbutyric acid (PBA) and the database for the prediction of miRNA targets. (**b**) mRNA expression of *Jun* and *Mcl-1* in AGS cells transfected with *miR-512-5p* precursor molecules (miR-512) and negative control (NC) was analysed by quantitative reverse transcriptase–PCR. The expression level was normalized to the *GAPDH* RNA expression level and expressed as mean + s.d. $*P<0.05$, $**P<0.01$ compared with negative control. (**c**) The protein expression level of Mcl-1 was analysed by western blotting in AGS cells not treated (NT) or treated with 5Aza-CdR and PBA (AP), as well as in AGS cells transfected with *miR-512-5p* precursor molecules (miR-512) and negative control (NC). β-actin is used as a loading control. (**d**) Levels of cytoplasmic histone-associated DNA fragments (mono- and oligonucleosomes) in AGS cells after transfection of *miR-512-5p* and after treatment with 5-Aza-CdR and PBA. Values are expressed as mean + s.d. $*P<0.05$ compared with negative control or untreated cells. GAPDH, glyceraldehydes 3-phosphate dehydrogenase.